nature chemistry

SUPPLEMENTARY INFORMATION

DOI: 10.1038/NCHEM.2712

In the format provided by the authors and unedited.

Cooperative polymerization of α-helices induced by macromolecular architecture

Ryan Baumgartner[1], Hailin Fu[2], Ziyuan Song[3], Yao Lin[2]*, and Jianjun Cheng[1,3]*

[1]Department of Chemistry, University of Illinois at Urbana-Champaign, Urbana, Illinois 61801, USA
[2]Department of Chemistry, University of Connecticut, Storrs, Connecticut 06269, USA
[3]Department of Materials Science, University of Illinois at Urbana-Champaign, Urbana, Illinois 61801, USA

*Corresponding Authors
Yao Lin: yao.lin@uconn.edu
Jianjun Cheng: jianjunc@illinois.edu

Table of Contents

I. General Considerations

General Experimental Details

All reagents and solvents were purchased from Sigma-Aldrich and used as received unless otherwise specified. γ-Benzyl-L-glutamic acid, γ-Benzyl-D-glutamic acid, and γ-Ethyl-L-glutamic acid were purchased from Chem-Impex. All polymerizations were mixed in an MBraun glovebox under argon. Dichloromethane (DCM) was prepared by refluxing over CaH_2 for 24 h distilling, and purging with nitrogen gas for 15 minutes. Dry hexanes and THF were prepared by passing nitrogen purged solvents through activated alumina columns. All dry solvents were stored over 4Å sieves in the glovebox. All vials used to handle trimethylsilyl (TMS) protected amines were silanzed by allowing vials to sit over vapor of chlorotrimethylsilane for 4 h in a desiccator under static vacuum. Vials were rinsed with deionized water, dried at 100°C, and stored in the glovebox. Grubbs catalyst (G3),[1] *N*-tritylethylenediamine,[2] and EG_2-Lys-NCA[3] were synthesized according to literature procedures. All kinetic experiments were performed with the same batch of NCA monomer.

Instrumentation

Nuclear magnetic resonance (NMR) spectra were recorded on a Varian U400, VXR500, or U500 NMR spectrometer. Chemical shifts are referenced to residual protons in the deuterated NMR solvents. MestReNova 8.1.1 was used to analyze all spectra. Fourier transform infrared (IR) spectra were performed using a Spectrum 100 spectrometer (Perkin Elmer) in a SL-3 Model 0.1 mm KBr permanent sealed liquid cell (International Crystal Laboratories). Gel Permeation Chromatography (GPC) was performed on a system equipped with a Model 1200 isocratic pump (Agilent Technology) in series with a 717 Autosampler (Waters) and size exclusion columns (10^2 Å, 10^3 Å, 10^4 Å, 10^5 Å, 10^6 Å Phenogel columns, 5 µm, 300 × 7.8 mm, Phenomenex) which were maintained at a temperature of 60°C. A DAWN HELEOS (Wyatt Technology) multiangle laser light scattering (MALLS) operating at a wavelength of 658 nm and an Optilab rEX refractive index detector (Wyatt Technology) operating at a wavelength of 658 nm were used as detectors. The mobile phase consisted of *N,N*-dimethylformamide (DMF) containing 0.1M LiBr at a flow rate of 1 mL min^{-1}. Samples were filtered through a 0.45 µm PTFE filter before analysis. Absolute molecular weights of polymers were determined using ASTRA 6.1.1.17 software (Wyatt Technology) and calculated from *dn/dc* values assuming 100% mass recovery. Circular Dichroism (CD) spectroscopy was conducted on a JASCO J-815 spectrometer in a quartz cell with a path length of 0.1 cm. Atomic force microscopy (AFM) images were taken under ambient conditions in tapping mode on a Cypher (Asylum Research) using BS-Tap 300Al tips (Budget Sensors). Solutions of polymers in DCM were diluted in DMF to a final concentration of 0.1 mg mL^{-1} and spin coated onto freshly cleaved mica at 4000 rpm under dry nitrogen for 2 minutes.

II. Procedures

γ-Benzyl-L-glutamate-*N*-carboxyanhydride (BLG-NCA).

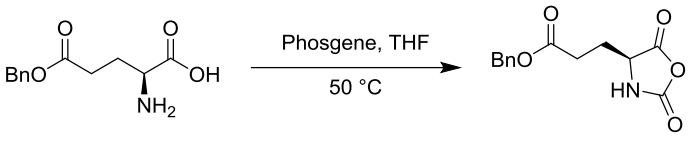

To an oven dried 250 mL round bottom flask was added γ-Benzyl-L-glutamic acid (6.03 g, 25.4 mmol), which was dried under high vacuum with stirring for 2 h. The flask was filled with nitrogen and 80 mL of dry THF was added to create a suspension. The flask was cooled on ice, then phosgene (15 wt% in toluene, 22.1 mL, 31.0 mmol) was added in one portion. The flask was then placed into a pre-warmed oil bath at 50 °C, heated for 2 h under nitrogen. The now clear, colorless solution was cooled and evaporated. The residue was transferred to a glovebox, dissolved in ca. 25 mL dry THF and recrystallized by layering 5-10 volumes of dry hexanes, and allowing to stand for 48 h. This procedure was repeated three times to yield a white crystalline solid (5.4 g, 81%). The D isomer was prepared in the same manner.

^{1}H NMR (500 MHz, $CDCl_3$): δ 7.41–7.29 (m, 5H), 6.94 (s, 1H), 5.12 (s, 2H), 4.38 (t, *J* = 6.2 Hz, 1H), 2.57 (t, *J* = 7.1, 2H), 2.25 (dq, *J* = 13.5, 6.7 Hz, 1H), 2.11 (dq, *J* = 14.2, 7.1 Hz, 1H). **^{13}C NMR** (125 MHz, $CDCl_3$): δ 172.5, 169.6, 152.2, 135.3, 128.8, 128.7, 128.4, 67.2, 57.0, 29.8, 27.0. **Anal. Calcd** for $C_{13}H_{13}NO_5$: C, 59.31; H, 4.98; N, 5.32. Found: C, 59.39; H, 4.75; N, 5.50.

γ-Ethyl-L-glutamate-*N*-carboxyanhydride (ELG-NCA).

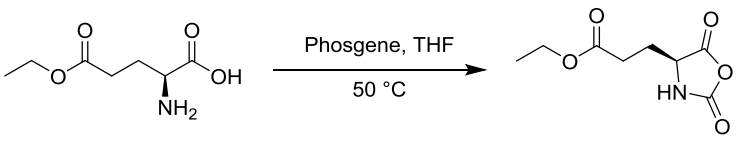

To an oven dried 250 mL round bottom flask was added γ-Ethyl-L-glutamic acid (6.0 g, 34.3 mmol), which was dried under high vacuum with stirring for 2 h. The flask was filled with nitrogen and 110 mL of dry THF was added to create a suspension. The flask was cooled on ice, then phosgene (15 wt% in toluene, 29.8 mL, 41.8 mmol) was added in one portion. The flask was then placed into a pre-warmed oil bath at 50 °C, heated for 2 h under nitrogen. The now clear, slightly yellow solution was cooled, evaporated, and transferred to a glovebox. The residue was dissolved in ca. 25 mL dry THF and recrystallized by layering 5-10 volumes of dry hexanes, and allowing to stand for 48 h. After the first recrystallization, the residue was dissolved in 25 mL THF, and filtered through a pad of dry celite to remove insoluble material. The resulting clear amber solution was then recrystallized twice more to yield long tan prisms solid (4.2 g, 61%). Monomer of exceptional quality for kinetic experiments was prepared by washing with DCM, then finally, dissolving in DCM and filtering through a pad of celite.

^{1}H NMR (500 MHz, $CDCl_3$): δ 6.83 (s, 1H), 4.42 (t, *J* = 6.1 Hz, 1H), 4.15 (dq, *J* = 7.1, 1.2 Hz, 2H), 2.54 (t, *J* = 7.2 Hz, 2H), 2.30–2.23 (m, 1H), 2.15–2.08 (m, 1H), 1.26 (td, *J* = 7.2, 1.2 Hz, 3H). **^{13}C NMR** (125 MHz, $CDCl_3$): δ 172.8, 169.6, 152.2, 61.5, 57.1, 29.9, 27.0, 14.2. **HRMS** (ESI-TOF) m/z: $[M + H]^+$ Calcd for $C_8H_{12}NO_5$ 202.0715; Found 202.0717.

(3a*R*,4*R*,7*S*,7a*S*)-2-benzyl-3a,4,7,7a-tetrahydro-1*H*-4,7-methanoisoindole-1,3(2*H*)-dione: (Ph)

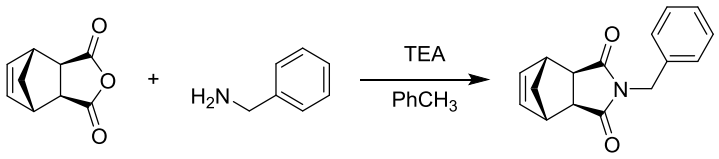

In a round bottom flask was added *cis*-norbornene-*exo*-2,3-dicarboxylic anhydride (500 mg, 3.05 mmol), pure distilled benzylamine (353 µL, 3.2 mmol), triethylamine (467 µL, 3.4 mmol), and 15 mL toluene. The reaction was refluxed under dean stark trap overnight. After cooling the reaction, 20 mL ethyl acetate was added and the reaction was washed with 3 x 10 mL 1N HCl, 10 mL brine, dried over Na_2SO_4, and dried *in vacuo*. The product was recrystallized from ice cold methanol to yield 425 mg of brilliant white crystalline product (55% yield).

^{1}H NMR (500 MHz, $CDCl_3$): δ 7.39–7.27 (m, 5H), 6.27 (t, *J* = 1.8 Hz, 2H), 4.62 (s, 2H), 3.25 (p, *J* = 1.8 Hz, 2H), 2.68 (d, *J* = 1.4 Hz, 2H), 1.41 (dp, *J* = 9.9, 1.6 Hz, 1H), 1.06 (dt, *J* = 10.0, 1.5 Hz, 1H). **^{13}C NMR** (125 MHz, $CDCl_3$): δ 177.8, 138.1, 136.0, 129.0, 128.8, 128.1, 48.0, 45.4, 42.8, 42.5. **HRMS** (ESI-TOF) m/z: $[M + H]^+$ Calcd for $C_{16}H_{16}NO_2$ 254.1181; Found 254.1173.

Synthetic Scheme of NB

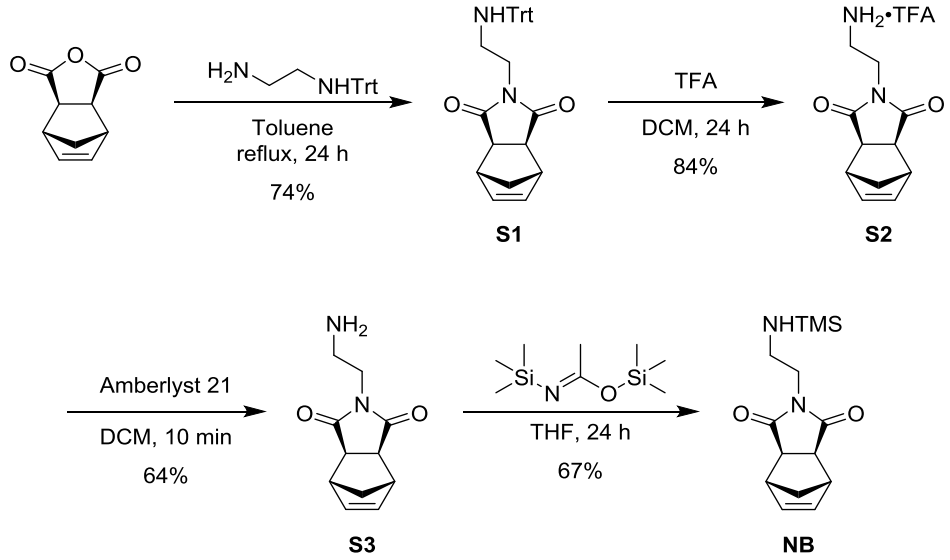

(3a*R*,4*R*,7*S*,7a*S*)-2-(2-(tritylamino)ethyl)-3a,4,7,7a-tetrahydro-1*H*-4,7-methanoisoindole-1,3(2*H*)-dione: (S1)

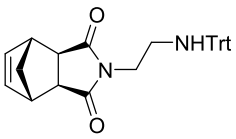

The reaction was carried out similar to previous procedures.[4] Briefly, a solution of *N*-tritylethylenediamine (9.15 g, 30.3 mmol) and *cis*-5-norbornene-*exo*-2,3-dicarboxylic anhydride (3.35 g, 20.4 mmol) in dry toluene (50 mL) was refluxed for 24h. The reaction mixture was evaporated, dissolved in 100 mL DCM and washed twice with 1N HCl (50 mL), followed by 50 mL saturated bicarbonate solution, 50 mL water, and 50 mL brine. The organic layer was dried over Na_2SO_4 and evaporated to yield a white/tan powder. Product was recrystallized from a large amount of methanol to give 6.8 g of **S1** as a white microcrystalline powder (74% yield).

^{1}H NMR (500 MHz, DMSO-d_6): δ 7.34 (d, *J* = 7.5 Hz, 6H), 7.27 (t, *J* = 7.7 Hz, 6H), 7.18 (tt, *J* = 7.3, 1.5 Hz, 3H), 6.29 (t, *J* = 1.5 Hz, 2H), 3.52 (t, *J* = 6.7 Hz, 2H), 3.08 (d, *J* = 2.9 Hz, 2H), 2.88 (t, *J* = 7.9 Hz, 1H), 2.68 (s, 2H), 2.13 (q, *J* = 7.1 Hz, 2H), 1.31 (d, *J* = 9.8 Hz, 1H), 1.12 (d, 9.6 Hz, 1H). **^{13}C NMR** (125 MHz, $CDCl_3$): δ 178.3, 145.8, 137.9, 128.5, 127.9, 126.4, 70.7, 48.0, 45.3, 43.0, 41.9, 39.1. **HRMS** (ESI-TOF) m/z: $[M + H]^+$ Calcd for $C_{30}H_{29}N_2O_2$ 449.2229; Found 449.2224.

(3a*R*,4*R*,7*S*,7a*S*)-2-(2-aminoethyl)-3a,4,7,7a-tetrahydro-1*H*-4,7-methanoisoindole-1,3(2*H*)-dione trifluoroacetate: (S2)

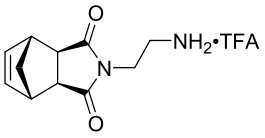

A solution of **S1** (2.76 g, 6.15 mmol) was dissolved in 12 mL DCM. Trifluoroacetic acid (2.37 mL, 31 mmol) was added dropwise and the resulting solution was capped and stirred overnight at room temperature. The resulting solution was evaporated and 30 mL ether was added to precipitate the product. Filtration of the suspension provided 1.65 g of **S2** as a white powder (84% yield).

^{1}H NMR (500 MHz, DMSO-d_6): δ 7.90 (s, 3H), 6.32 (t, *J* = 1.7 Hz, 2H), 3.63 (t, *J* = 6.3 Hz, 2H), 3.10 (s, 2H), 2.96 (t, *J* = 6.4 Hz, 2H), 2.69 (d, *J* = 1.3 Hz, 2H), 1.35 (d, *J* = 9.8 Hz, 1H), 1.20 (d, *J* = 9.8 Hz, 1H). **^{13}C NMR** (125 MHz, DMSO-d_6): δ 177.7, 137.7, 47.6, 44.5, 42.7, 36.6, 35.7. **^{19}F NMR** (470 MHz, DMSO-d_6): δ -74.1. **HRMS** (ESI-TOF) m/z: $[M + H]^+$ Calcd for $C_{11}H_{15}N_2O_2$ 207.1134; Found 207.1134.

(3a*R*,4*R*,7*S*,7a*S*)-2-(2-((trimethylsilyl)amino)ethyl)-3a,4,7,7a-tetrahydro-1*H*-4,7-methanoisoindole-1,3(2*H*)-dione: (NB)

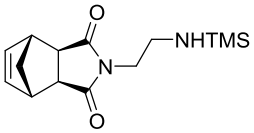

The trifluoroacetate salt **S2** (1.07 g, 3.35 mmol) was dissolved into 10 mL DCM resulting in a cloudy solution. Amberlyst A21 free base resin (2.7 g) was added to the solution and stirred for 10 minutes. The solution became clear, and then slightly turbid. The reaction was filtered through a small pipet of celite and evaporated immediately to obtain 441 mg (2.14 mmol, 64% yield) of a light yellow oily residue which solidified into a white powder upon scratching. Product (**S3**) is unstable at room temperature in solid and solution state for long periods of time. Following isolation the product was transferred to a glovebox and used immediately in the next step without additional purification.

In a glovebox, **S3** (441 mg, 2.14 mmol) was added to a solution of *N*,*O*-bis(trimethylsilyl)acetamide (1.05 mL, 4.28 mmol) in 5 mL of dry THF and allowed to stir overnight. The solution was transferred to a dry narrow schlenk tube and carefully evaporated at room temperature to yield an oil. The schlenk tube was then transferred outside the glovebox and immersed in a 50 °C oil bath for 2-3 h under high vacuum to sublime the crystalline mono silylated acetamide byproduct along the sides of the flask. The reaction was transferred back into the glovebox and dry THF was carefully added to dissolve and remove the residue remaining at the bottom of the schlenk tube containing the desired product. To the resulting THF solution (ca. 5 mL) of product was added more *N*,*O*-bis(trimethylsilyl)acetamide (105 µL, 0.43 mmol) and stirred overnight. The solution was evaporated *in vacuo* at room temperature and the resulting residue was recrystallized from dry hexanes at -30 °C three times to yield 398 mg of **NB** as a white crystalline powder (1.43 mmol, 67% yield).

^{1}H NMR (500 MHz, $CDCl_3$): δ 6.28 (t, *J* = 1.9 Hz, 2H), 3.47 (t, *J* = 6.6 Hz, 2H), 3.26 (p, *J* = 1.6 Hz, 2H), 2.89 (dt, *J* = 8.1, 6.6 Hz, 2H), 2.67 (d, *J* = 1.4 Hz, 2H), 1.49 (dp, *J* = 9.8, 1.6 Hz, 1H), 1.35 (dtd, *J* = 9.8, 1.7, 0.9 Hz, 1H), 0.41 (t, *J* = 8.1 Hz, 1H), 0.00 (s, 9H). **^{13}C NMR** (125 MHz, $CDCl_3$): δ 178.5, 137.9, 48.0, 45.3, 43.0, 42.0, 39.6, 0.0. **Anal. Calcd** for $C_{14}H_{22}N_2O_2Si$: C, 60.39; H, 7.96; N, 10.06. Found: C, 60.38; H, 7.68; N, 10.17.

Sample polymerization of linear poly(γ-Benzyl-L-glutamate)

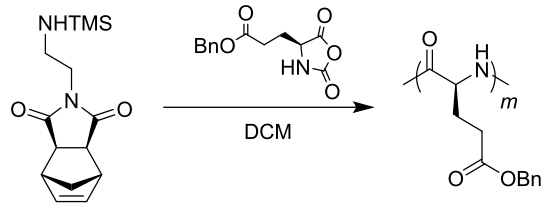

In a silanzed 2 mL Reacti-Vial™ was placed BLG-NCA (26.3 mg, 0.1 mmol) with a magnetic stir vane. The solid was dissolved in DCM, and NB (10 mg mL^{-1} in DCM) was added at the proper [M]:[I] ratio ensuring the final concentration of [M] = 0.5 M. The reaction was capped tightly and stirred at room temperature overnight. After the polymerization, solvent was evaporated and the remaining polymer was dissolved in GPC mobile phase and injected into the GPC without additional purification.

Capping of PNB with Boc_2O (PNBBoc)

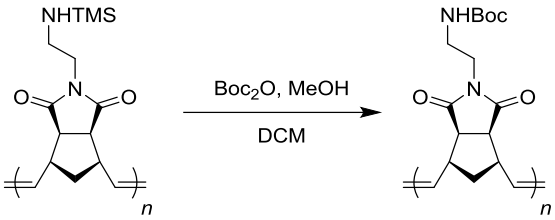

Since PNB is unstable under ambient conditions, it is necessary to remove the TMS group and protect the resulting amine before GPC analysis can be conducted. In the glovebox, di-*tert*-butyl dicarbonate (15 equiv to TMS) was added to the polymer solution. Then, methanol (100 equiv to TMS) was quickly added under stirring. The solution was stirred for 1 hour, removed from the glovebox, and precipitated into 4 mL ether three times to yield a white solid. (*dn/dc* = 0.0824)

Typical ozonolysis of PBLG polymers

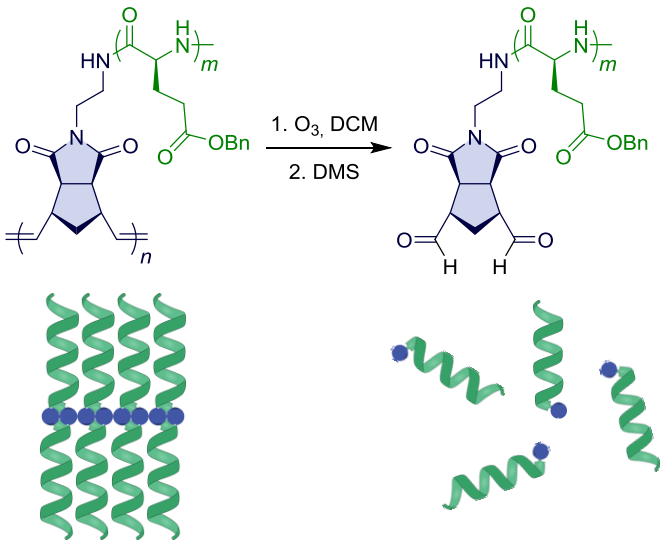

A stream of oxygen was passed through a solution/suspension of linear or brush PBLG (ca. 25.0 mg) in DCM (ca. 4 mL) cooled to -78 °C for 2 min. The ozone generator was then turned on and ozone was bubbled through the chilled solution for 15 min to ensure complete degradation of the brush polymer. The solution became blue after 2-3 min. After ozone treatment, oxygen was bubbled through the solution for 2-3 min, until the solution became colorless. To the resulting solution was added 100 µL of dimethyl sulfide (DMS). The reaction was then allowed to sit overnight at room temperature. Unfractionated polymers were analyzed by GPC by directly drying *in vacuo*. Polymers could alternatively be isolated through precipitation of the concentrated solution into methanol. Yields were typically > 75 %. The ^{1}H NMR is identical to that of native linear PBLG.

III. Supplementary Figures and Tables

A. Polynorbornene Backbone (PNB) Characterization

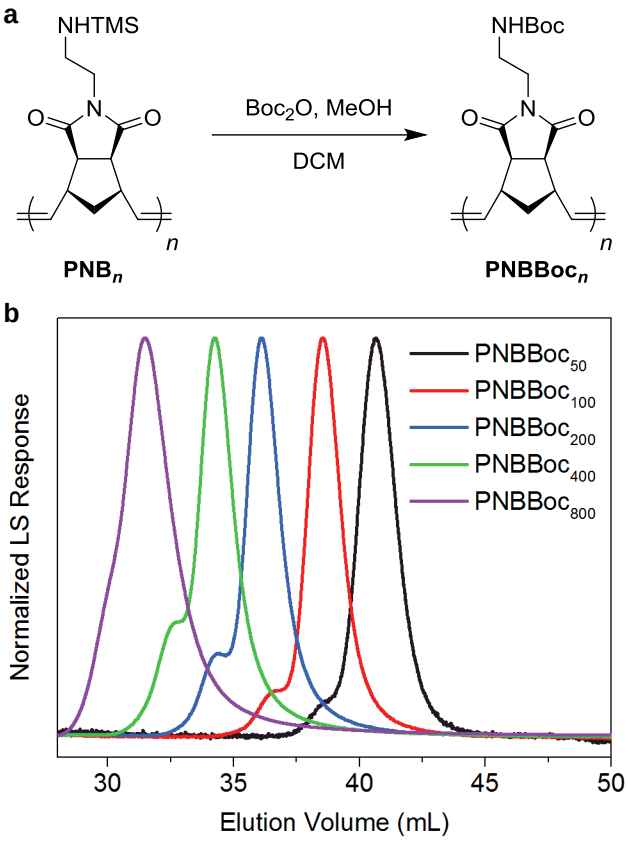

Supplementary Figure 1 | Backbone molecular weight characterization. a,b, Synthetic scheme (**a**) and LS GPC traces (**b**) of PNBBoc$_n$ protected polymers at varying degrees of polymerization. Protection was necessary as PNB polymers crosslinked overtime when removed from the glovebox. The shoulder peak at lower elution volume is likely due to a small residual amount of crosslinking which occurs during capping of the amine. See Supplementary Table 1.

Supplementary Table 1 | PNBBoc$_n$ polymer characterization

Polymer	[M]:[I]	M_n[a] (M_n*) kDa	M_w/M_n[a]
PNBBoc$_{50}$	50	15.6 (15.4)	1.021
PNBBoc$_{100}$	100	31.0 (30.6)	1.014
PNBBoc$_{200}$	200	66.4 (61.4)	1.051
PNBBoc$_{400}$	400	149 (123)	1.096
PNBBoc$_{800}$	800	345 (245)	1.126

Polymerizations performed in DCM with [M] = 0.02 M. Reactions were polymerized for 18 minutes / 100 monomers. [a] Determined via gel permeation chromatography; M_n* = expected molecular weight; *dn/dc* = 0.0824.

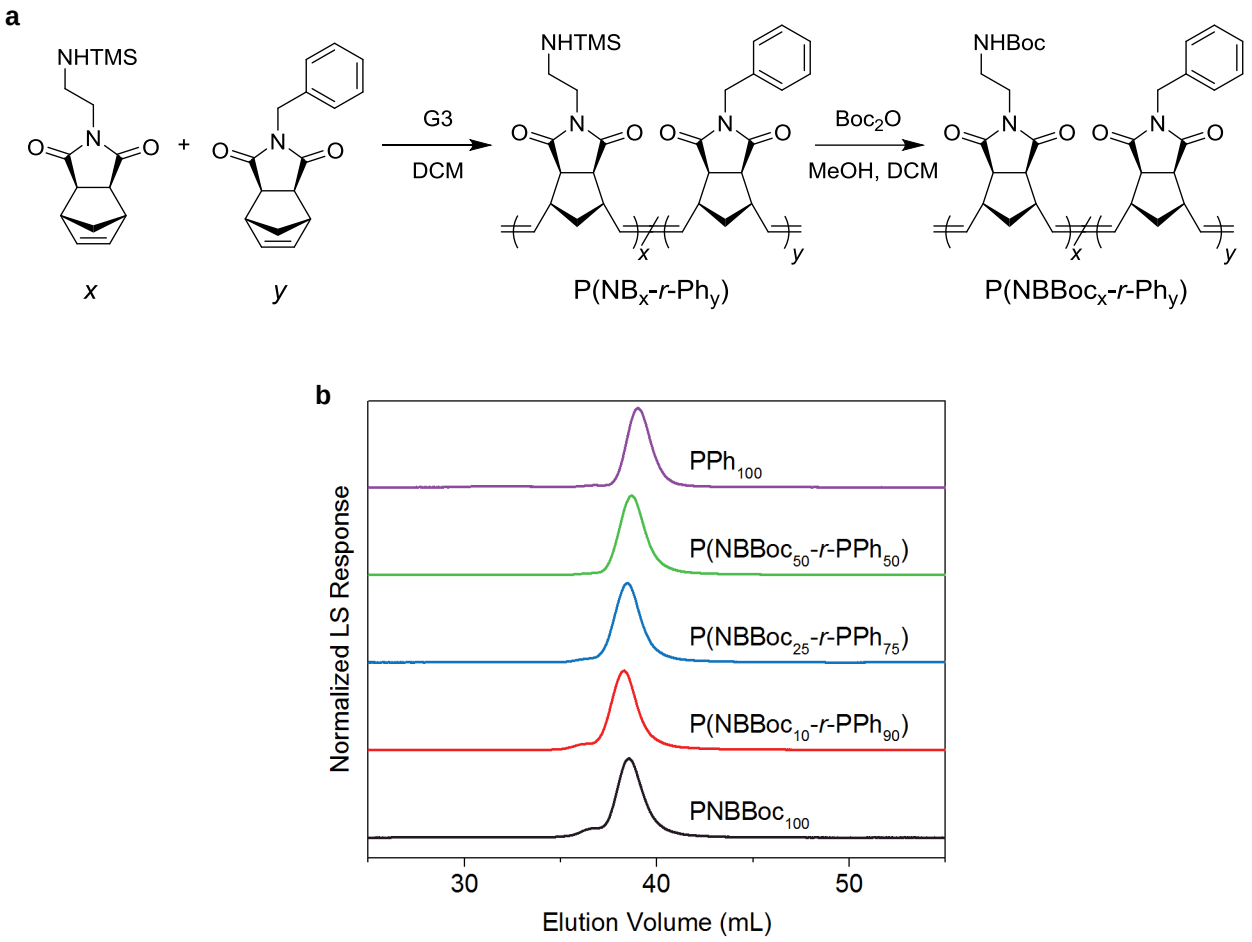

Supplementary Figure 2 | Random copolymer backbone characterization. a,b, Synthetic scheme (**a**) and GPC traces (**b**) of P(NBBoc$_x$-*r*-Ph$_y$) random copolymers. See Supplementary Table 2.

Supplementary Table 2 | Random copolymer characterization

Polymer	M_n[a] (M_n*) kDa	M_w/M_n[a]	dn/dc[a]	x:y[b]
PNBBoc$_{100}$	31.0 (30.8)	1.01	0.0842	--
P(NBBoc$_{50}$-*r*-Ph$_{50}$)	29.1 (28.1)	1.02	0.1125	50:50
P(NBBoc$_{25}$-*r*-Ph$_{75}$)	27.9 (26.8)	1.02	0.1232	26:74
P(NBBoc$_{10}$-*r*-Ph$_{90}$)	26.7 (26.0)	1.01	0.1370	10:90
PPh$_{100}$	25.7 (25.5)	1.01	0.1396	--

Polymerizations performed in DCM with [M] = 0.02 M. Reactions were polymerized for 16 minutes. [a] Determined via gel permeation chromatography; [b] Determined from ^{1}H NMR M_n* = expected molecular weight.

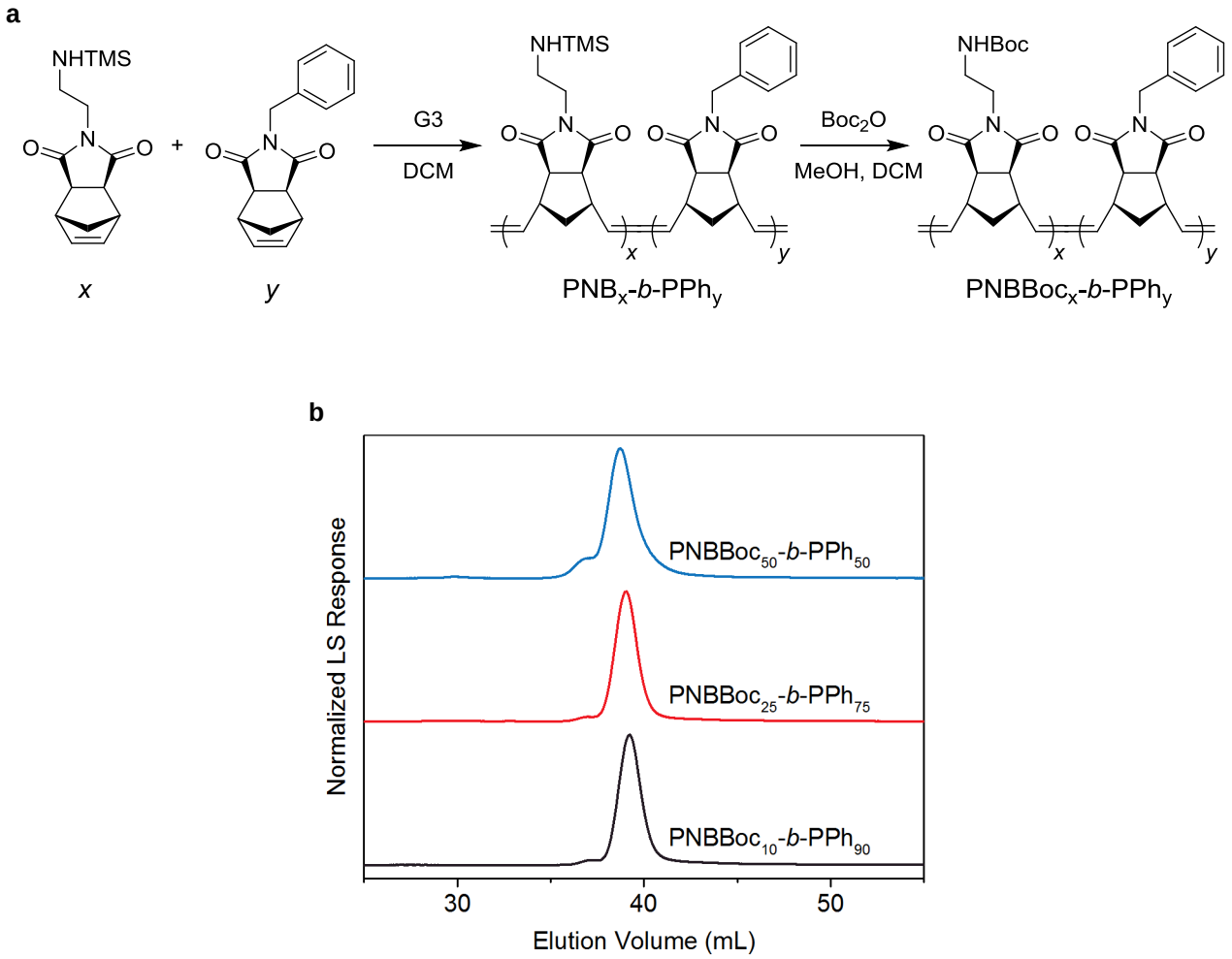

Supplementary Figure 3 | Block copolymer backbone characterization. a,b, Synthetic scheme (**a**) and GPC traces (**b**) of PNBBoc$_x$-*b*-PPh$_y$ copolymers. See Supplementary Table 3.

Supplementary Table 3 | Block copolymer characterization

Polymer	M_n[a] (M_n*) kDa	M_w/M_n[a]	*dn/dc*[a]	*x*:*y*[b]
PNBBoc$_{50}$-*b*-PPh$_{50}$	22.6 (28.1)	1.05	0.1125	47:53
PNBBoc$_{25}$-*b*-PPh$_{75}$	21.5 (26.8)	1.01	0.1232	27:73
PNBBoc$_{10}$-*b*-PPh$_{90}$	20.8 (26.0)	1.01	0.1370	9:11

Polymerizations performed in DCM with [M] = 0.02 M. Reactions were polymerized for 16 minutes.
[a] Determined via gel permeation chromatography; [b] Determined from ^{1}H NMR M_n* = expected molecular weight.

B. Brush Polymer Characterization

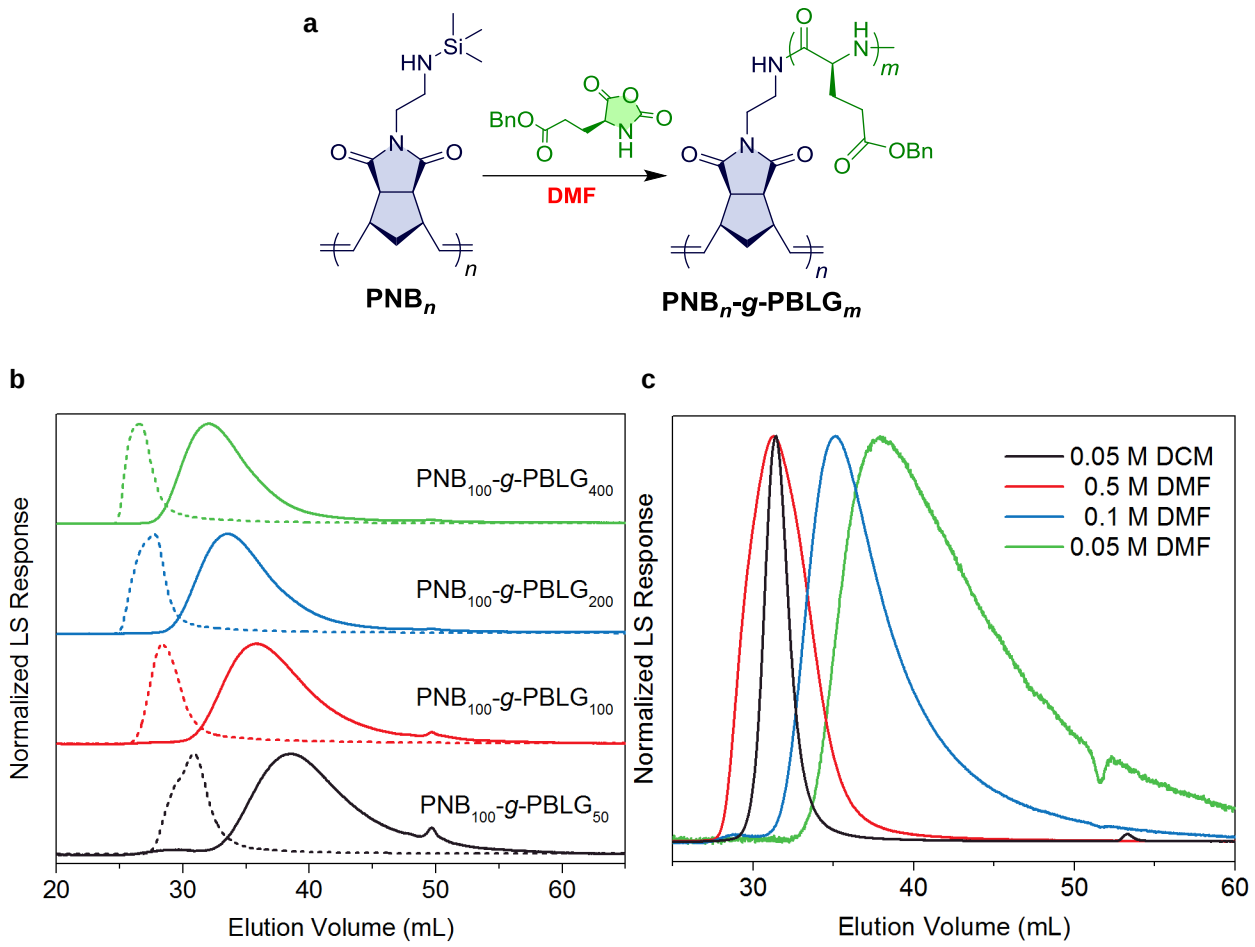

Supplementary Figure 4 | Characterization of brush polymers in DMF. a, Scheme of brush polymerization in DMF. **b,** GPC LS traces of PBLG based brush polymers initiated from PNB$_{100}$ in DMF before (dashed) and after (solid) backbone degradation via ozonolysis. [NCA] for polymerization = 0.5 M (See Supplementary Table 4). **c,** GPC LS traces of PNB$_{50}$-*g*-PBLG$_{50}$ brush polymers synthesized at varying concentrations in DCM or DMF after 48 h.

Supplementary Table 4 | PBLG based brush polymer characterization (DMF)

Brush Polymer					Ozonolysis Product	
Polymer	**M_n[a] (M_n*) MDa**	**M_w/M_n[a]**	**% Conv. (48 h)[b]**	**GD (%)[c]**	**M_n[a] (M_n*) kDa**	**M_w/M_n[a]**
PNB$_{100}$-*g*-PBLG$_{50}$	1.5 (1.10)	1.13	95	44	24.8 (11.0)	1.34
PNB$_{100}$-*g*-PBLG$_{100}$	3.8 (2.18)	1.22	95	56	39.5 (21.8)	1.37
PNB$_{100}$-*g*-PBLG$_{200}$	9.5 (4.34)	1.69	90	59	74.5 (43.4)	1.28
PNB$_{100}$-*g*-PBLG$_{400}$	14.8 (8.68)	2.52	69	62	142 (86.6)	1.20

Polymerizations performed in DMF with [M] = 0.5 M. Reactions were polymerized for 48 h. [a] Determined via gel permeation chromatography; M_n* = expected molecular weight. [b] Determined via IR [c] Grafting density (GD) of polymer chains calculated from following equation: GD = M_n* / M_n where M_n* is the theoretical molecular weight of the cleaved linear polymer and M_n is the measured molecular weight of the cleaved linear polymer.

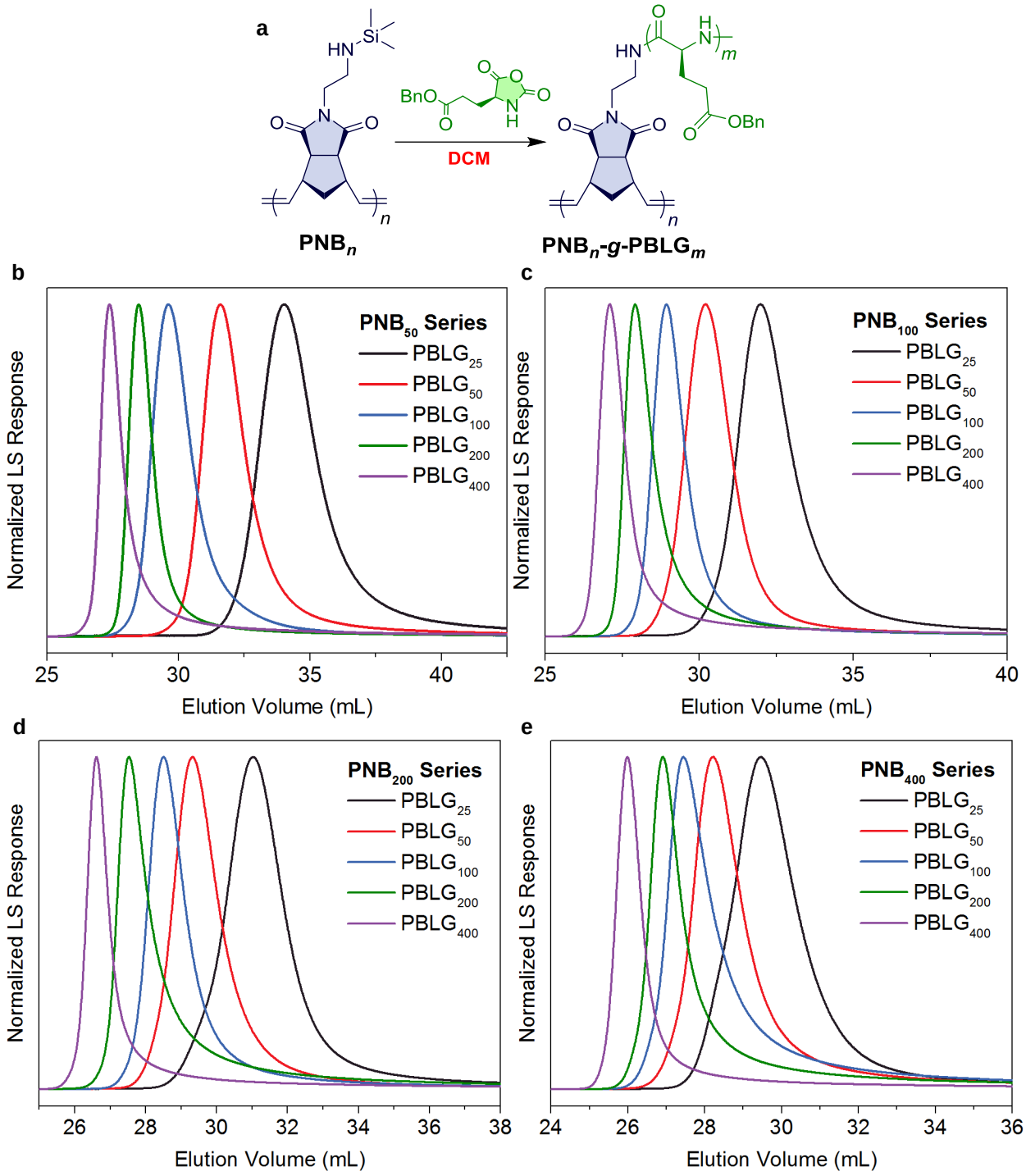

Supplementary Figure 5 | Characterization of brush polymers synthesized in DCM. a-e, GPC traces of brush polymers synthesized in DCM (**a**) at [M] = 0.05 M initiated from PNB_{50} (**b**), PNB_{100} (**c**), PNB_{200} (**d**), or PNB_{400} (**e**).

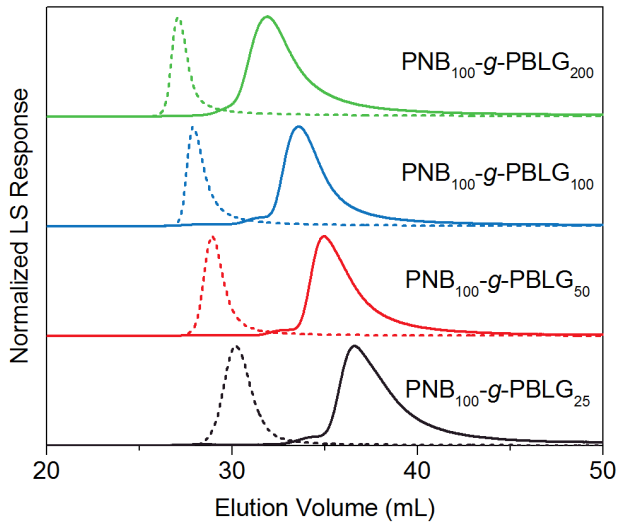

Supplementary Figure 6 | Ozonolysis of brush polymers. GPC LS traces of brush polymers initiated from PNB_{100} in DCM before (dashed) and after (solid) ozonolysis. [NCA] for polymerization = 0.05 M. See Supplementary Table 6.

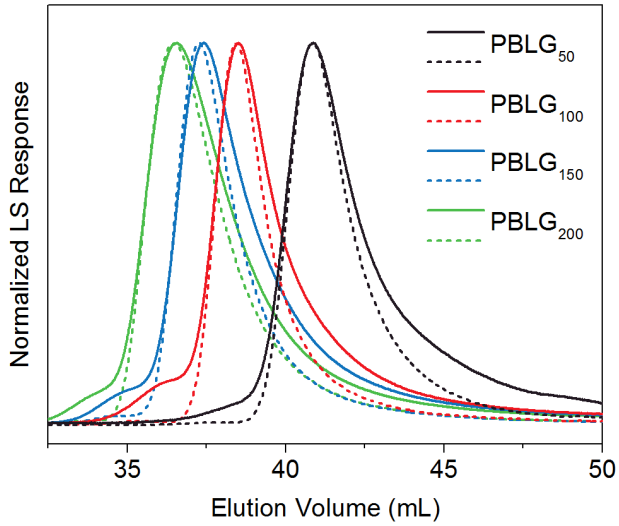

Supplementary Figure 7 | Stability of PBLG during ozonolysis. GPC LS traces of linear PBLG polymers before (dashed) and after (solid) ozonolysis demonstrating the integrity of PBLG during ozone treatment. See Supplementary Table 5.

Supplementary Table 5 | Stability of linear PBLG during ozonolysis

	Before Ozonolysis		After Ozonolysis		
Polymer	**M_n (kDa)[a]**	**M_w/M_n[a]**	**M_n (kDa)[a]**	**M_w/M_n[a]**	**Change (%)**
$PBLG_{50}$	22.1	1.04	23.2	1.03	4.9
$PBLG_{100}$	34.8	1.05	36.6	1.05	5.2
$PBLG_{150}$	41.4	1.08	45.1	1.05	8.9
$PBLG_{200}$	50.9	1.07	54.0	1.06	6.1

[a] Determined via gel permeation chromatography.

Supplementary Table 6 | PBLG brush polymer characterization (DCM)

Brush Polymer			Ozonolysis Product		
Polymer	**M_n[a] (M_n*) MDa**	**M_w/M_n[a]**	**M_n[a] (M_n*) kDa**	**M_w/M_n[a]**	**GD (%)[b]**
PNB_{50}-*g*-$PBLG_{25}$	0.27 (0.28)	1.03	31.0 (5.6)	1.14	18
PNB_{100}-*g*-$PBLG_{25}$	0.58 (0.56)	1.05	28.0 (5.6)	1.27	20
PNB_{200}-*g*-$PBLG_{25}$	1.23 (1.12)	1.05	--	--	--
PNB_{400}-*g*-$PBLG_{25}$	2.59 (2.24)	1.08	--	--	--
PNB_{10}-*g*-$PBLG_{50}$	0.14 (0.11)	1.13	48.1 (11.0)	1.05	23
PNB_{50}-*g*-$PBLG_{50}$	0.61 (0.55)	1.02	60.1 (11.0)	1.01	19
PNB_{100}-*g*-$PBLG_{50}$	1.25 (1.10)	1.02	65.5 (11.0)	1.03	17
PNB_{200}-*g*-$PBLG_{50}$	2.53 (2.20)	1.04	62.6 (11.0)	1.04	18
PNB_{400}-*g*-$PBLG_{50}$	5.79 (4.40)	1.07	--	--	--
PNB_{10}-*g*-$PBLG_{100}$	0.25 (0.22)	1.11	82.6 (21.8)	1.05	27
PNB_{50}-*g*-$PBLG_{100}$	0.97 (1.09)	1.02	--	--	--
PNB_{100}-*g*-$PBLG_{100}$	2.29 (2.18)	1.02	88.8 (21.8)	1.03	25
PNB_{200}-*g*-$PBLG_{100}$	4.18 (4.36)	1.02	84.0 (21.8)	1.04	26
PNB_{400}-*g*-$PBLG_{100}$	11.15 (8.72)	1.06	--	--	--
PNB_{10}-*g*-$PBLG_{200}$	0.50 (0.43)	1.08	126 (43.4)	1.05	35
PNB_{50}-*g*-$PBLG_{200}$	2.03 (2.17)	1.01	138 (43.4)	1.04	30
PNB_{100}-*g*-$PBLG_{200}$	4.23 (4.34)	1.01	134 (43.4)	1.03	33
PNB_{200}-*g*-$PBLG_{200}$	8.29 (8.68)	1.02	131 (43.4)	1.03	34
PNB_{400}-*g*-$PBLG_{200}$	22.3 (17.36)	1.08	--	--	--
PNB_{50}-*g*-$PBLG_{400}$	4.09 (4.33)	1.02	207 (86.6)	1.04	40
PNB_{100}-*g*-$PBLG_{400}$	7.94 (8.66)	1.03	193 (86.6)	1.05	46
PNB_{200}-*g*-$PBLG_{400}$	16.60 (17.32)	1.03	197 (86.6)	1.05	45
PNB_{400}-*g*-$PBLG_{400}$	43.33 (34.64)	1.07	--	--	--

Polymerizations performed in DCM with [M] = 0.05 M. Monomer conversion for all polymerizations was > 98% as measured by IR. [a] Determined via gel permeation chromatography; M_n* = expected molecular weight. [b] Grafting density (GD) of polymer chains calculated from following equation: GD = M_n* / M_n where M_n* is the theoretical molecular weight of the cleaved linear polymer and M_n is the measured molecular weight of the cleaved linear polymer.

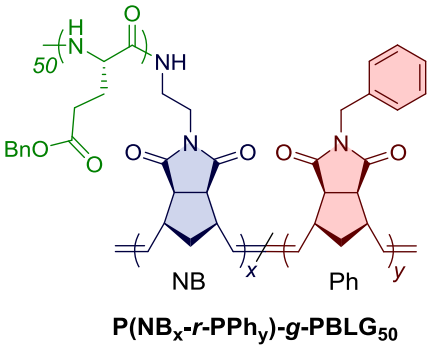

P(NB$_x$-*r*-PPh$_y$)-*g*-PBLG$_{50}$

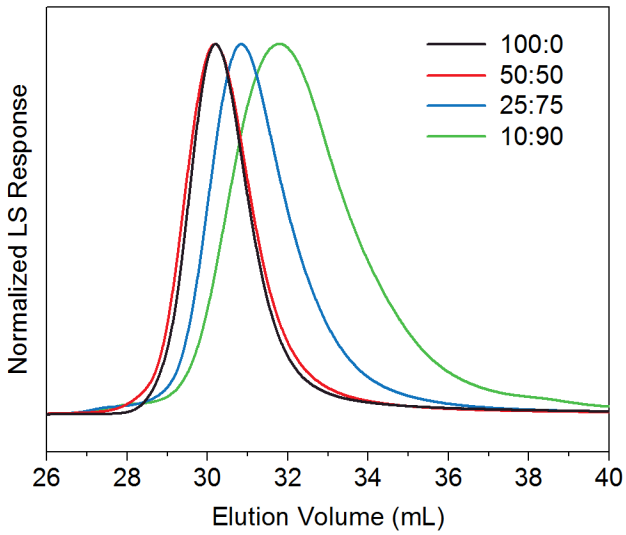

Supplementary Figure 8 | Molecular weight characterization of random copolymer brushes. GPC LS traces of P(NB$_x$-*r*-Ph$_y$)-*g*-PBLG$_{50}$ brush polymers. Ratios in legend are *x*:*y*. Backbone DP = *x*+*y*. See Supplementary Table 7.

Supplementary Table 7 | Characterization of P(NB$_x$-*r*-Ph$_y$)-*g*-PBLG$_{50}$ brush polymers

Brush Polymer			Ozonolysis Product		
Ratio *x*:*y*	**M_n[a] (M_n*) MDa**	**M_w/M_n[a]**	**M_n[a] (M_n*) kDa**	**M_w/M_n[a]**	**GD (%)[b]**
100:0	1.25 (1.10)	1.02	65.5 (11.0)	1.03	17
50:50	0.74 (0.57)	1.06	51.5 (11.0)	1.07	11
25:75	0.40 (0.30)	1.11	58.0 (11.0)	1.02	5
10:90	0.18 (0.13)	1.23	66.9 (11.0)	1.05	2

Polymerizations performed in DCM with [M] = 0.05 M. Monomer conversion for all polymerizations was > 98% as measured by IR. [a] Determined via gel permeation chromatography; M_n* = expected molecular weight. [b] Grafting density (GD) of polymer chains calculated from following equation: GD = (M_n* / M_n) × F_x where M_n* is the theoretical molecular weight of the cleaved linear polymer, M_n is the measured molecular weight of the cleaved linear polymer, and F_x = is the fraction of NB monomer contained in the backbone.

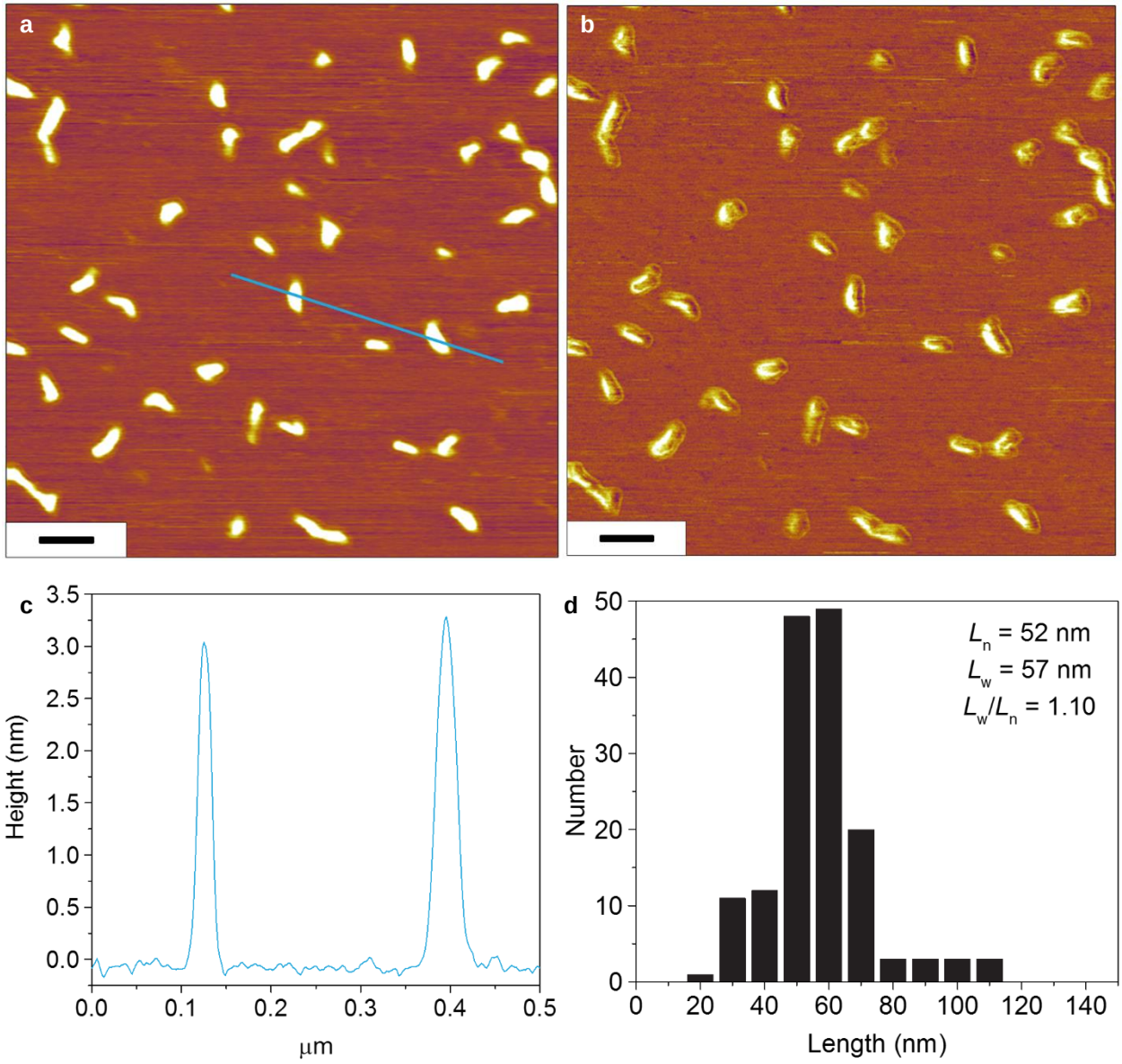

Supplementary Figure 9 | AFM analysis of PNB_{100}-*g*-$PBLG_{50}$. a-d, Height (**a**), and phase (**b**) micrographs. Line profile (**c**) and length distribution (**d**) of brushes (*n* = 153). Scale bar = 100 nm.

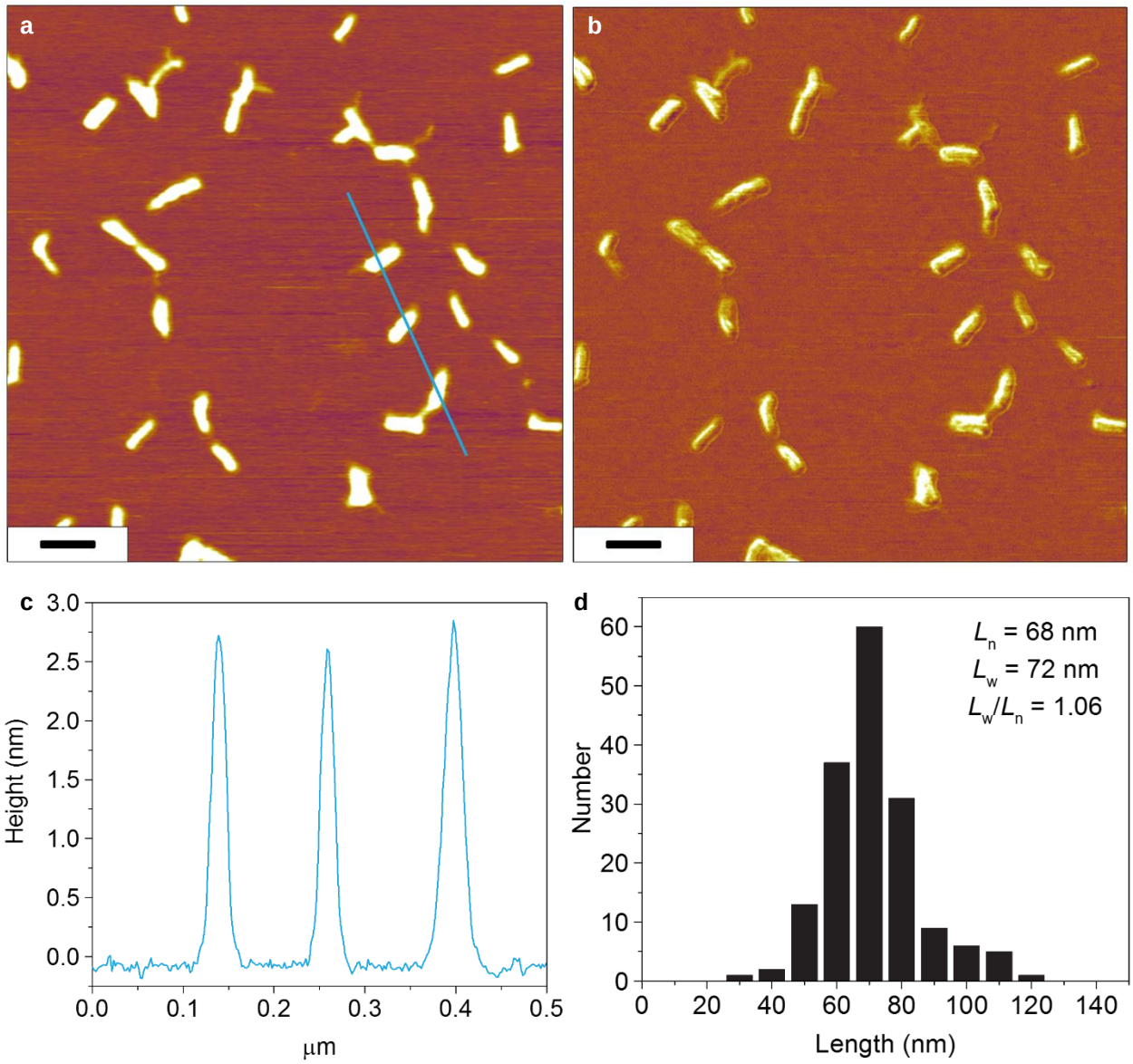

Supplementary Figure 10 | AFM analysis of PNB_{200}-*g*-$PBLG_{50}$. a-d, Height (**a**), and phase (**b**) micrographs. Line profile (**c**) and length distribution (**d**) of brushes (*n* = 169). Scale bar = 100 nm.

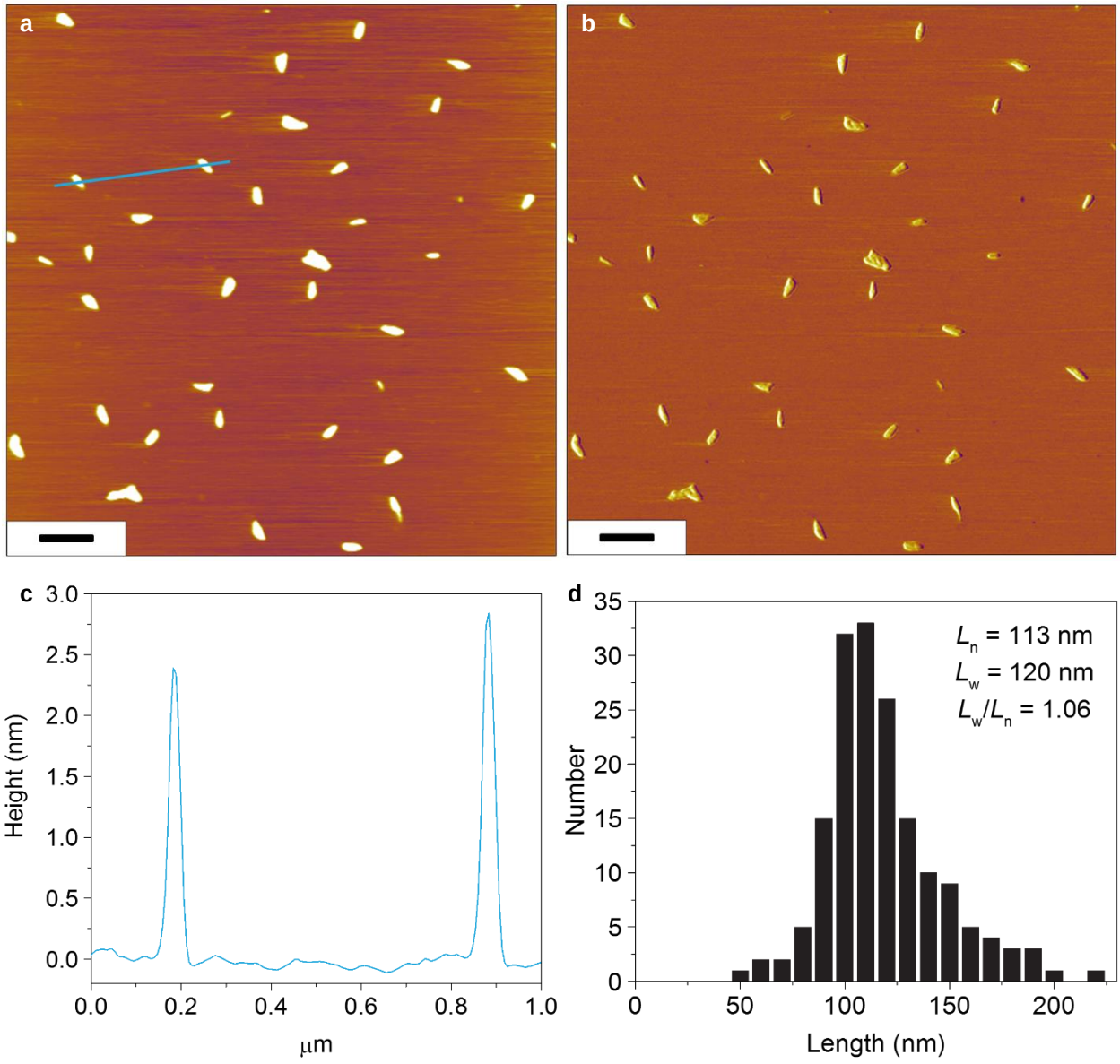

Supplementary Figure 11 | AFM analysis of PNB_{400}-*g*-$PBLG_{50}$. a-d, Height (**a**), and phase (**b**) micrographs. Line profile (**c**) and length distribution (**d**) of brushes (*n* = 167). Scale bar = 300 nm.

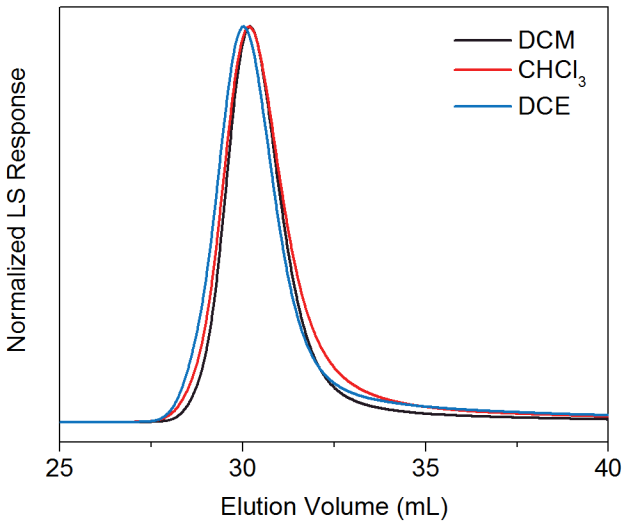

Supplementary Figure 12 | Brush polymer synthesized in various solvents. GPC LS traces of PNB_{100}-*g*-$PBLG_{50}$ polymers synthesized in various solvents. DCM = dichloromethane; $CHCl_3$ = chloroform, DCE = 1,2-dichloroethane.

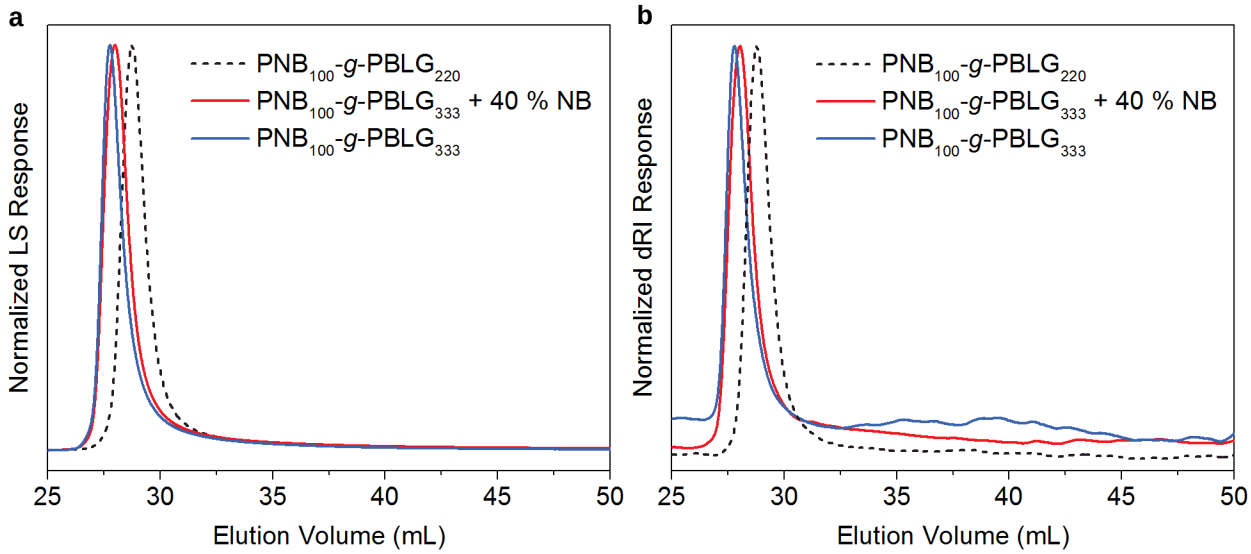

Supplementary Figure 13 | Brush polymerization in presence of linear initiator. a,b, GPC LS (**a**) and dRI (**b**) traces of PNB_{100} based brush polymers of various side chain lengths. The red trace is that of PNB_{100} mixed with 40 mol% of the linear initiator (NB). If the initiation and propagation of PNB_{100} and NB are equivalent, the MW of the brush polymer should be identical to PNB_{100}-*g*-$PBLG_{220}$ (dotted trace). The absence of lower molecular weight species further confirms that polymerization of PNB_{100} can occur in the presence of NB without the formation of linear byproducts.

C. Kinetic Data and Fitting

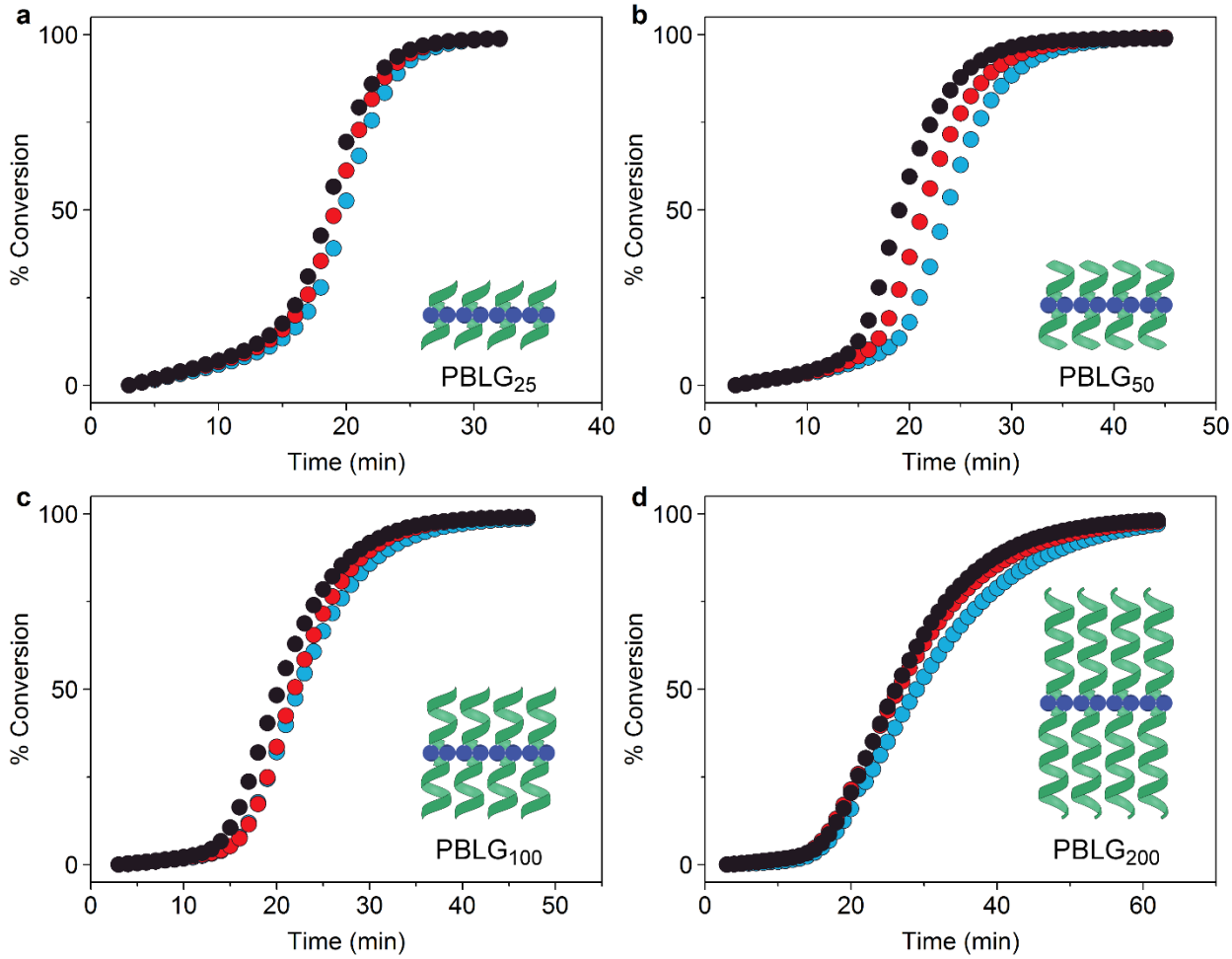

Supplementary Figure 14 | Kinetics of brush polymerization. a-d, Conversion of BLG-NCA in DCM as measured by IR after initiation with PNB_{100}. [NHTMS] = 2.0 mM ($PBLG_{25}$) (**a**), 1.0 mM ($PBLG_{50}$) (**b**), 0.50 mM ($PBLG_{100}$) (**c**), or 0.25 mM ($PBLG_{200}$) (**d**). [NCA] = 0.05 M.

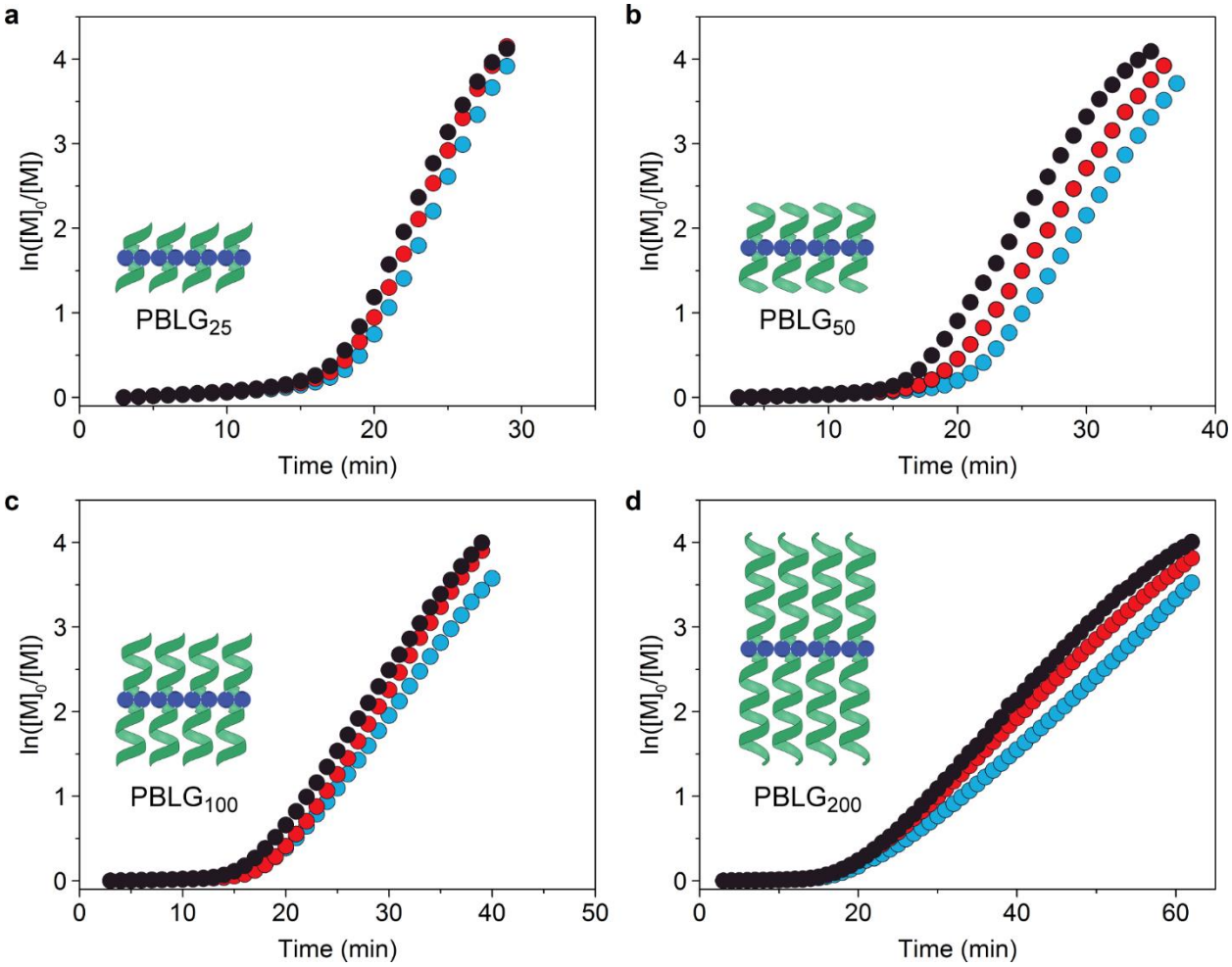

Supplementary Figure 15 | First-order plots of brush polymerization. a-d, Semilogarithmic plots of BLG-NCA in DCM as measured by IR after initiation with PNB_{100}. [NHTMS] = 2.0 mM ($PBLG_{25}$) (**a**), 1.0 mM ($PBLG_{50}$) (**b**), 0.5 mM ($PBLG_{100}$) (**c**), or 0.25 mM ($PBLG_{200}$) (**d**). [NCA] = 0.05 M.

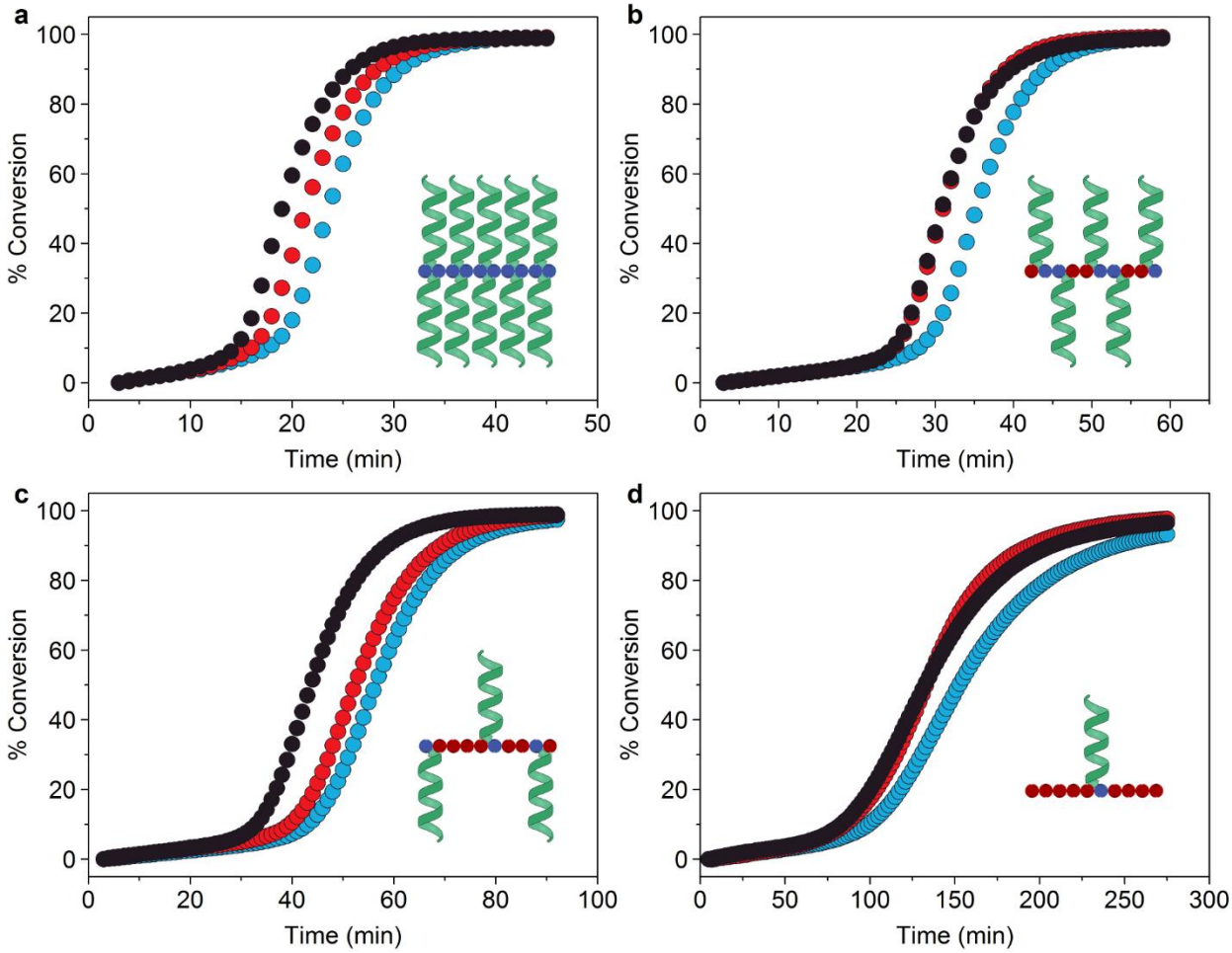

Supplementary Figure 16 | Kinetics of brush polymerization with random copolymer macroinitiators. a-d, Conversion of BLG-NCA in DCM as measured by IR after initiation with P(NB_x-*r*-Ph_y) random copolymers with *x*:*y* ratios of 100:0 (**a**), 50:50 (**b**), 25:75 (**c**), or 10:90 (**d**). *x*+*y* = DP; [NCA] = 0.05 M; [NHTMS] = 1.0 mM.

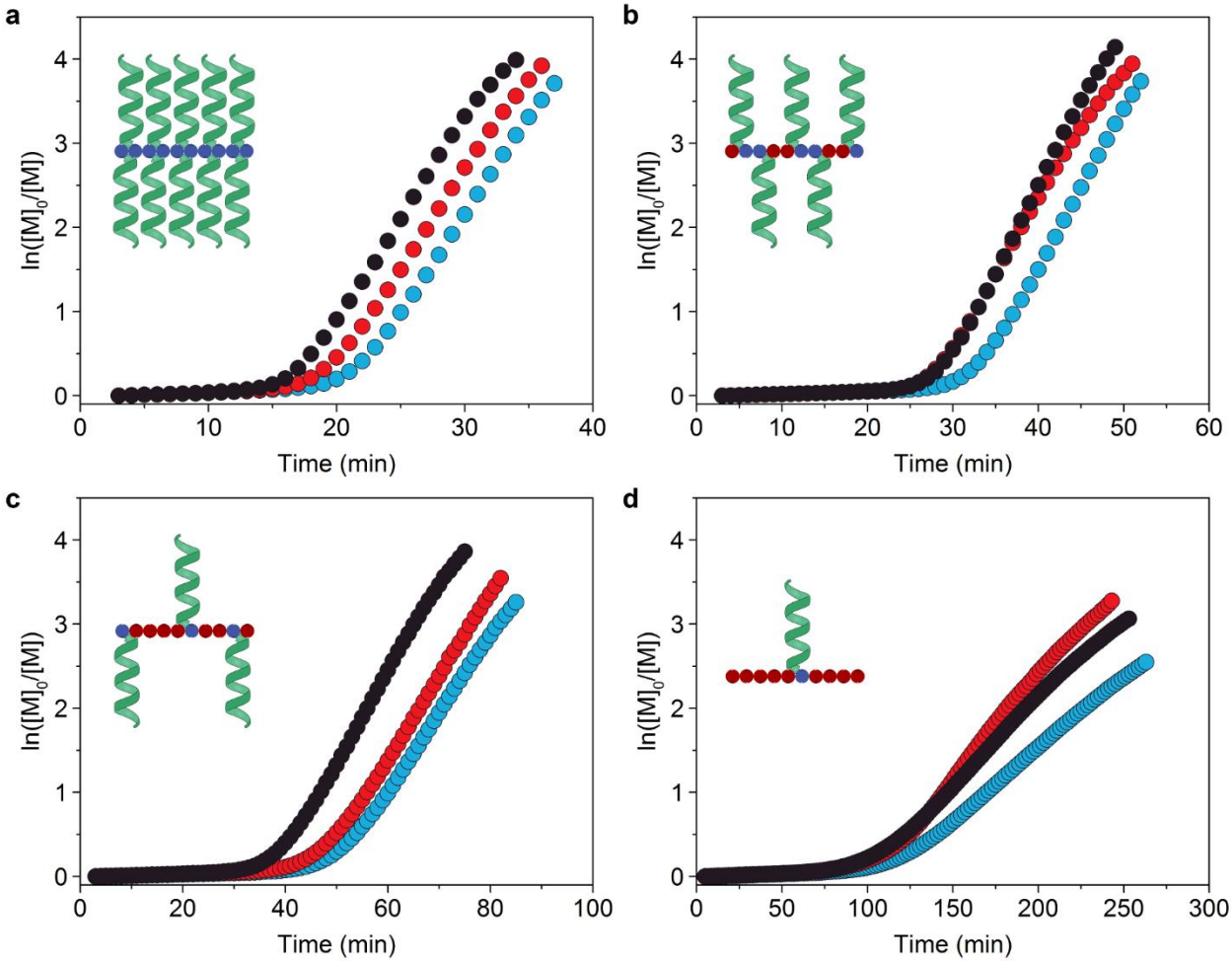

Supplementary Figure 17 | First-order plots of brush polymerization with random copolymer macroinitiators. a-d, Semilogarithmic plots of BLG-NCA in DCM as measured by IR after initiation with P(NB_x-*r*-Ph_y) random copolymers with *x*:*y* ratios of 100:0 (**a**), 50:50 (**b**), 25:75 (**c**), or 10:90 (**d**). *x*+*y* = DP; [NCA] = 0.05 M; [NHTMS] = 1.0 mM.

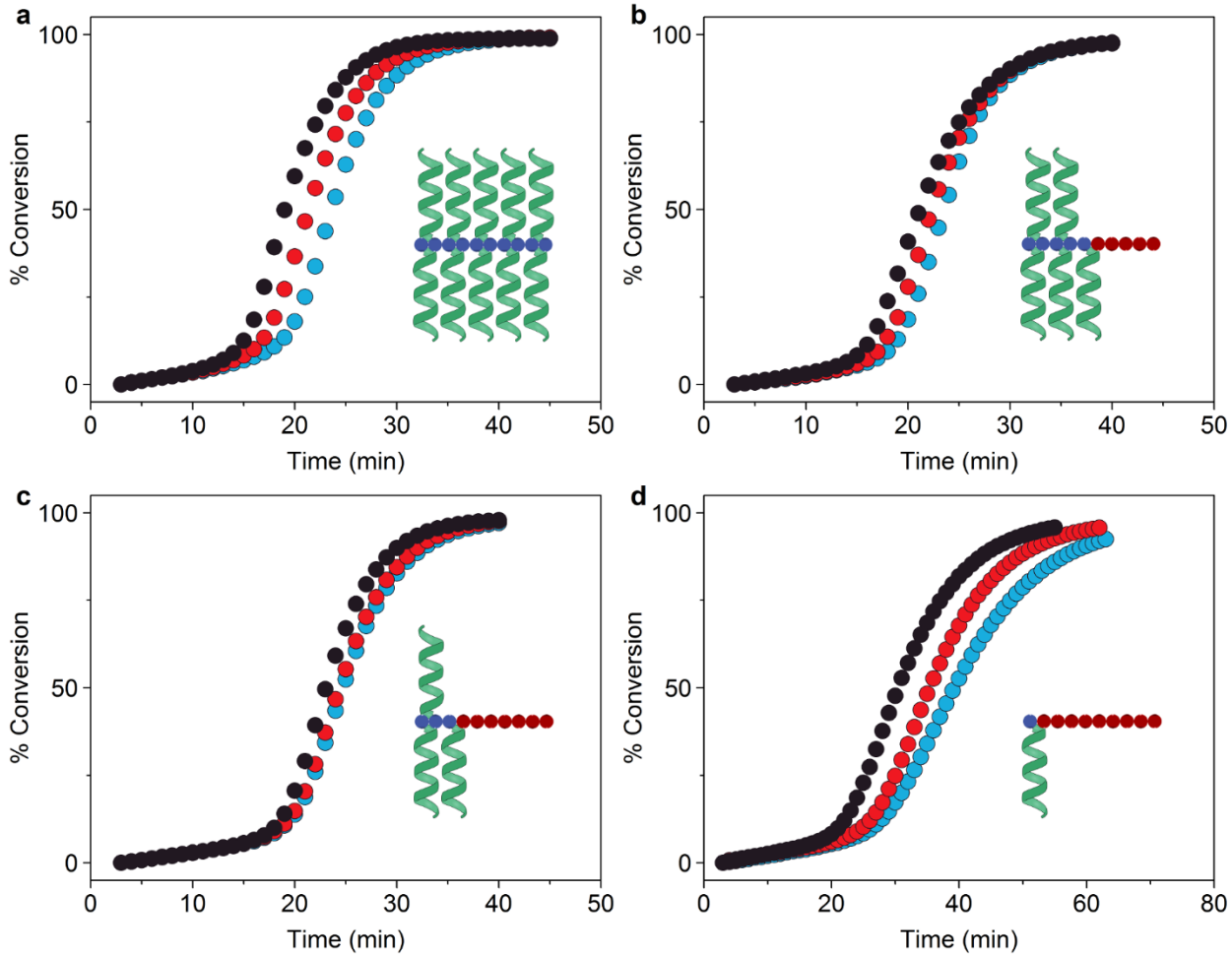

Supplementary Figure 18 | Kinetics of brush polymerization with block copolymer macroinitiators. a-d, Conversion of BLG-NCA in DCM as measured by IR after initiation with PNB_x-*b*-PPh_y block copolymers with *x*:*y* ratios of 100:0 (**a**), 50:50 (**b**), 25:75 (**c**), or 10:90 (**d**). *x*+*y* = DP; [NCA] = 0.05 M; [NHTMS] = 1.0 mM.

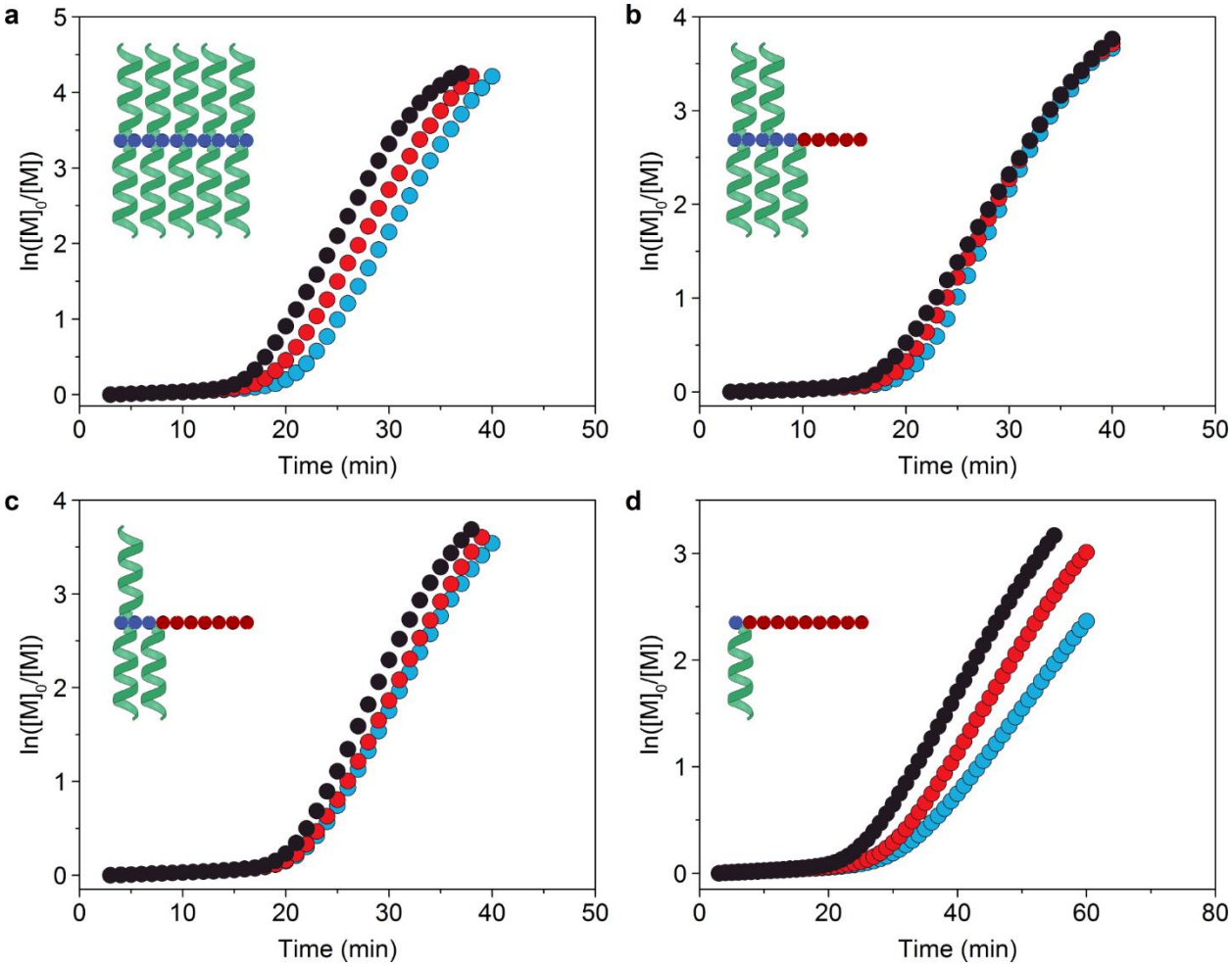

Supplementary Figure 19 | First-order plots of brush polymerization with block copolymer macroinitiators. a-d, Semilogarithmic plots of BLG-NCA in DCM as measured by IR after initiation with PNB_x-*b*-PPh_y block copolymers with *x*:*y* ratios of 100:0 (**a**), 50:50 (**b**), 25:75 (**c**), or 10:90 (**d**). *x*+*y* = DP; [NCA] = 0.05 M; [NHTMS] = 1.0 mM.

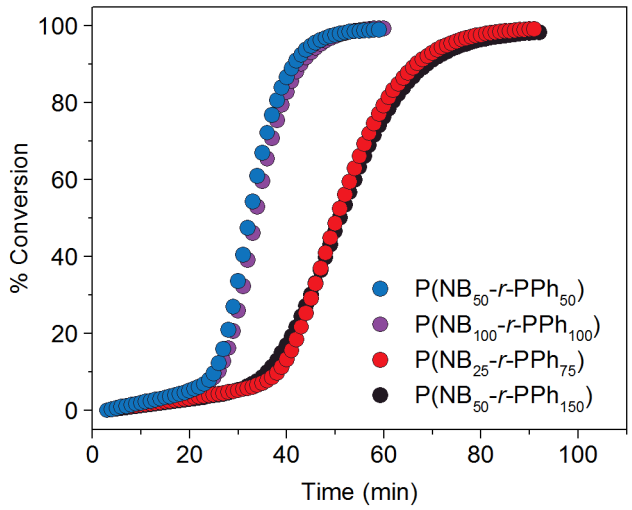

Supplementary Figure 20 | Dependence of polymerization rate on backbone length. Conversion of BLG-NCA after incubation with P(NB_x-*r*-Ph_y) random copolymer macroinitiators of varying composition and backbone length. The subscripts correspond to monomer composition where the sum of the subscripts is the total DP of the copolymer. [NCA] = 0.05 M; [NHTMS] = 1.0 mM.

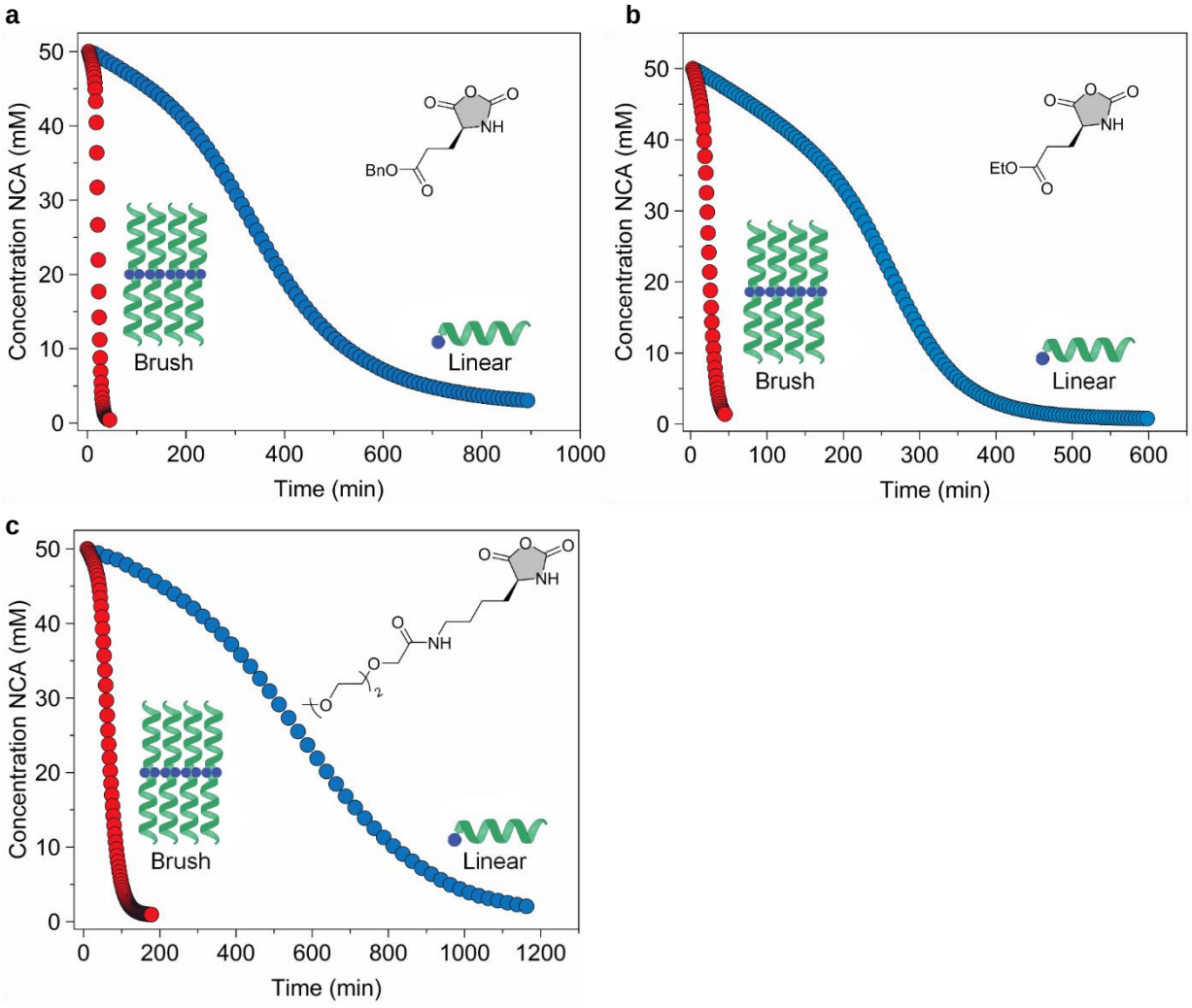

Supplementary Figure 21 | Kinetics of other NCA monomers. a-c, Conversion of BLG-NCA (**a**), ELG-NCA (**b**), or EG_2-Lys-NCA (**c**), in DCM after initiation with PNB_{100} (red) or **NB** (blue). [NCA] = 0.05 M; [NHTMS] = 1.0 mM.

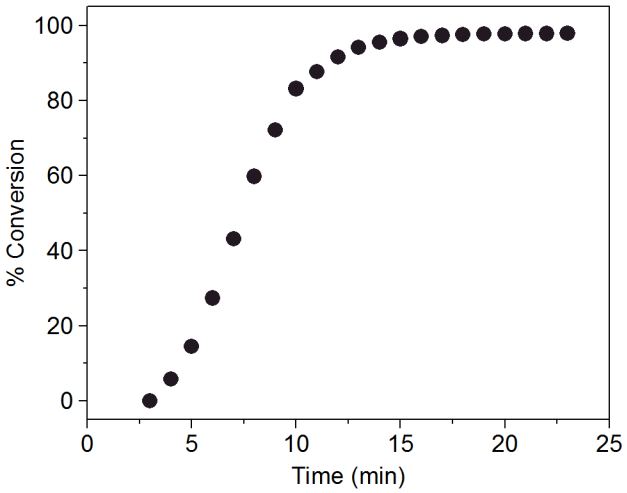

Supplementary Figure 22 | Kinetics in methylcyclohexane/chloroform. Polymerization kinetics of BLG-NCA initiated by PNB_{100} conducted in a 25:75 v/v mixture of methylcyclohexane:chloroform. Note that the plot contains a significant error due to the rapid nature of the polymerization and limitations in measuring data points before t = 3 min. The plot assumes 0% conversion at the first data point, however, the first stage (k_1) appears to be nearly complete by this time point. [NCA] = 0.05M; [NHTMS] = 1.0 mM.

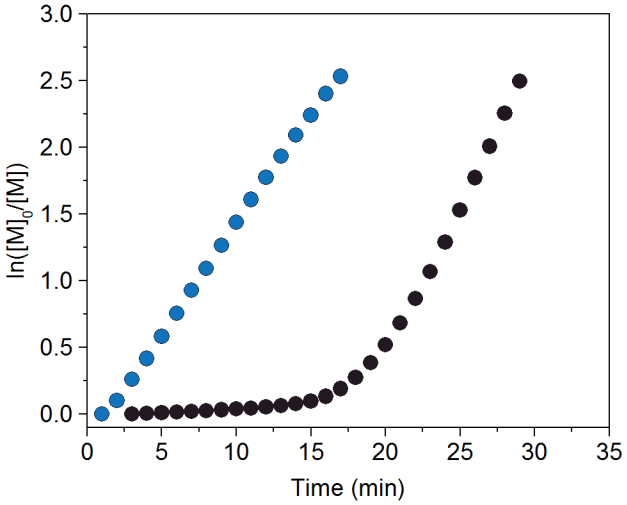

Supplementary Figure 23 | First-order plot after additional monomer. Semilogarithmic plot of BLG-NCA polymerization upon adding 50 equiv BLG-NCA to PNB_{100} (black), or to PNB_{100}-*g*-$PBLG_{50}$ (blue).

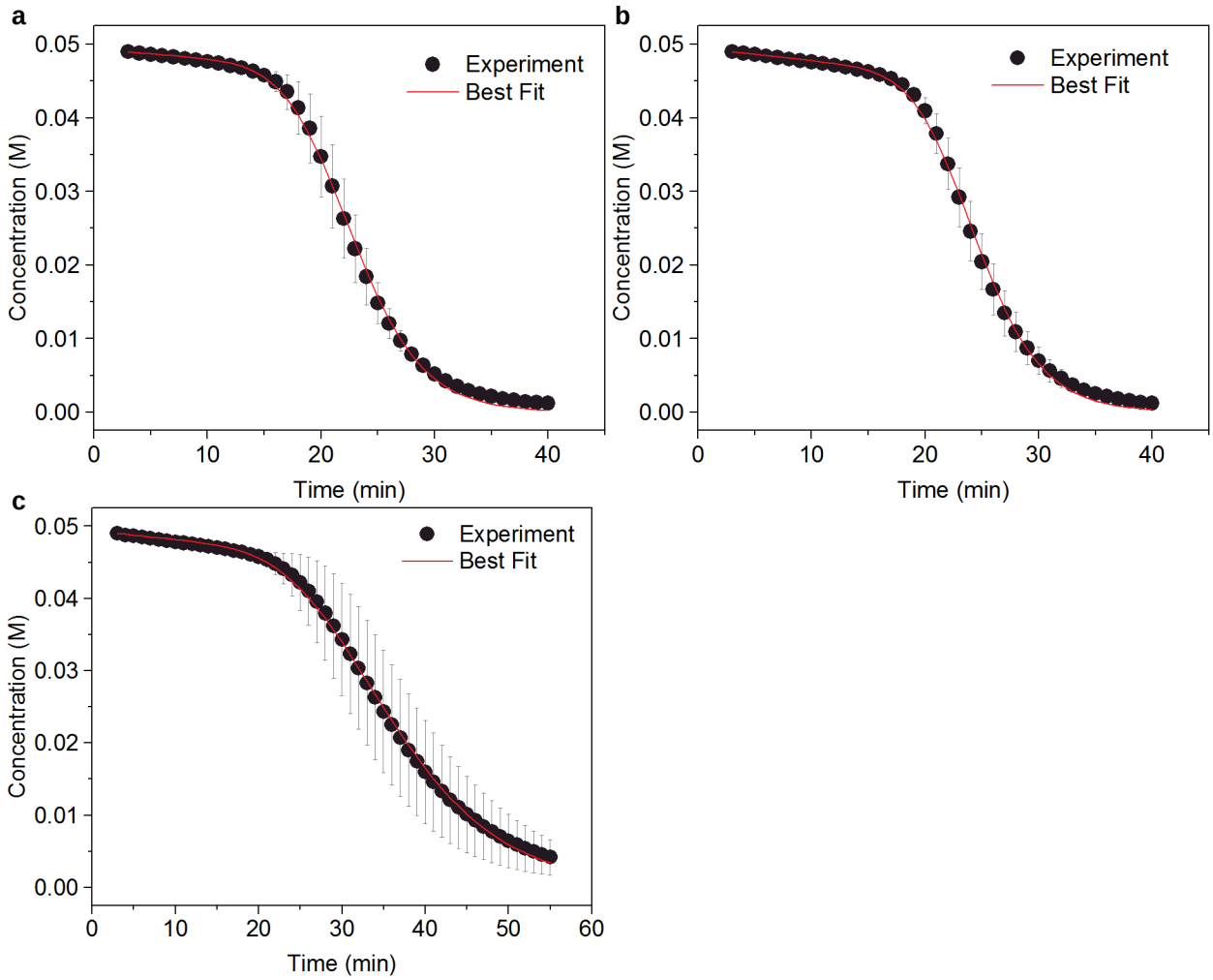

Supplementary Figure 24 | Kinetic fitting of polymerizations initiated from block copolymer macroinitiators. a-c, Kinetics for the polymerization of BLG-NCA in DCM initiated by PNB_{50}-*b*-PPh_{50} (**a**), PNB_{25}-*b*-PPh_{75} (**b**), or PNB_{10}-*b*-PPh_{90} (**c**). $[NCA]_0$ = 0.05 M, $[NHTMS]_0$ = 1.0 mM. Error bars represent standard deviations from three independent measurements.

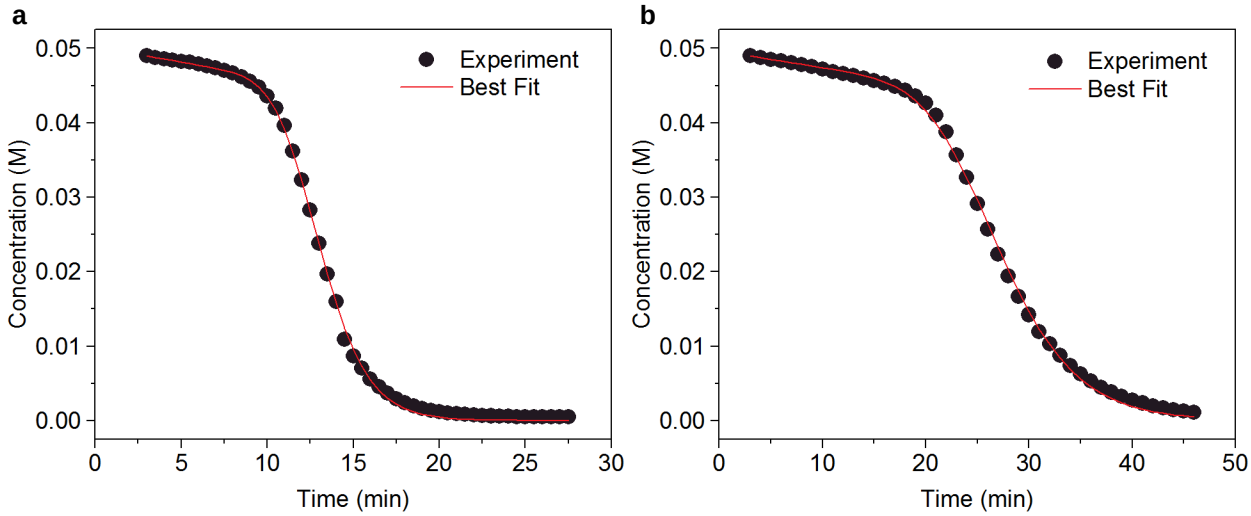

Supplementary Figure 25 | Kinetic fitting of polymerizations in various solvents. a-b, Polymerization of BLG-NCA initiated by PNB_{100} in chloroform (**a**), and 1,2-dichloroethane (**b**). [NCA] = 0.05 M, [NHTMS] = 1.0 mM.

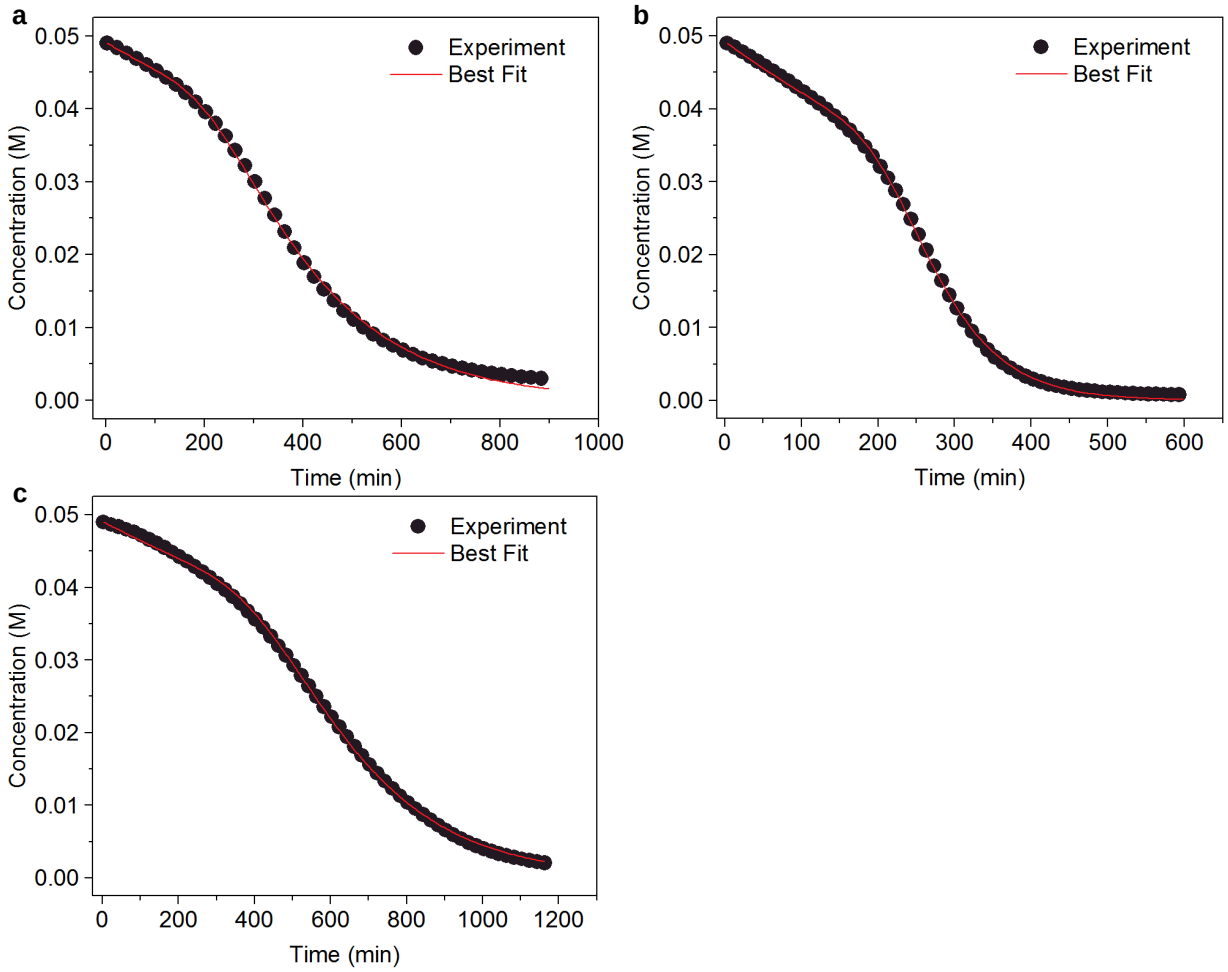

Supplementary Figure 26 | Linear polymerization kinetic fits of various monomers. a-c, Fits to linear polymerizations initiated by NB in DCM of BLG-NCA (**a**), ELG-NCA (**b**), and EG_2-Lys-NCA (**c**). [NCA] = 0.05 M, [NB] = 1.0 mM.

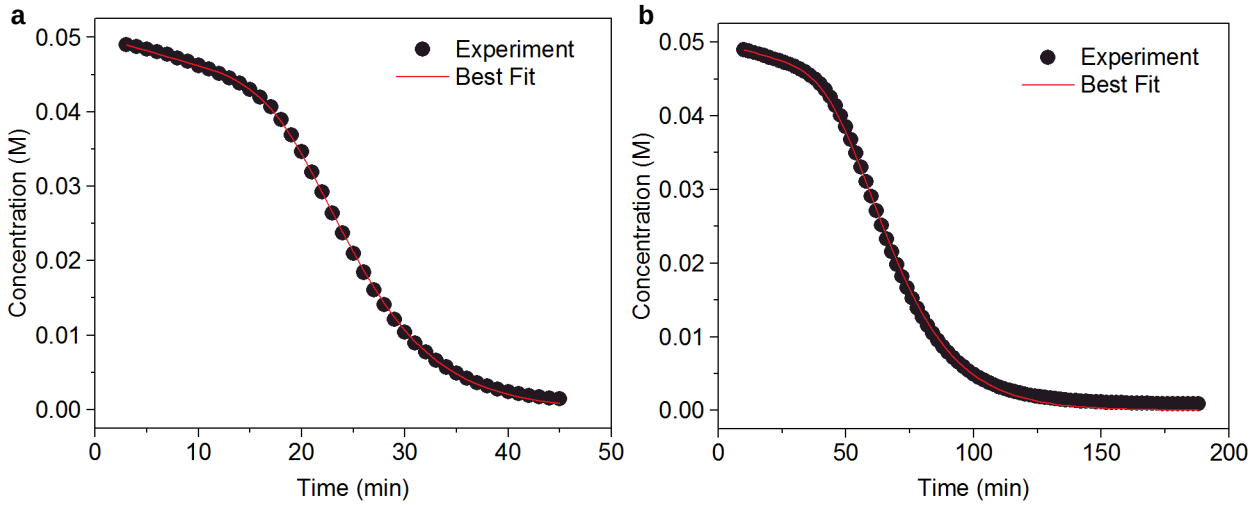

Supplementary Figure 27 | Brush polymerization kinetic fits of various monomers. a-b, Fits to brush polymerizations initiated by PNB_{100} in DCM of ELG-NCA (**a**) and EG_2-Lys-NCA (**b**). [NCA] 0.05 M, [NHTMS] = 1.0 mM.

Supplementary Table 8 | Rate constants from polymerizations

Polymer	k_1 (M^{-1} s^{-1})	k_2 (M^{-1} s^{-1})	*s*
PNB_{100}-*g*-$PBLG_{25}$	0.062	1480	10
PNB_{100}-*g*-$PBLG_{50}$	0.072	215	10
PNB_{100}-*g*-$PBLG_{100}$	0.129	25.5	10
PNB_{100}-*g*-$PBLG_{200}$	0.167	7.4	10
P(NB_{50}-*r*-Ph_{50})-*g*-$PBLG_{50}$	0.034	1260	10
P(NB_{25}-*r*-Ph_{75})-*g*-$PBLG_{50}$	0.034	39.2	10
P(NB_{10}-*r*-Ph_{90})-*g*-$PBLG_{50}$	0.020	1.2	10
(PNB_{50}-*b*-PPh_{50})-*g*-$PBLG_{50}$	0.053	121	8
(PNB_{25}-*b*-PPh_{75})-*g*-$PBLG_{50}$	0.062	294	10
(PNB_{10}-*b*-PPh_{90})-*g*-$PBLG_{50}$	0.054	7.3	8
PNB_{100}-*g*-$PELG_{50}$	0.14	5.9	10
PNB_{100}-*g*-P(EG_2-Lys)$_{50}$	0.034	1.71	7
[a] PNB_{100}-*g*-$PBLG_{50}$	0.142	417	10
[b] PNB_{100}-*g*-$PBLG_{50}$	0.081	32.5	10
$PBLG_{50}$	0.013	0.090	10
$PELG_{50}$	0.026	0.44	18
P(EG_2-Lys)$_{50}$	9.1×10^{-3}	8.5×10^{-2}	13

Polymerizations of NCA monomers were performed in DCM at [M] = 0.05 M. Rate constants and nucleation DP (*s*) were determined from best fits of the kinetic model. [a] Chloroform [b] 1,2-dichloroethane (DCE)

D. Dimensionless Equations of Kinetic Model

$$\tau = tk_1[M]_0 \qquad \sigma = \frac{k_1}{k_2} \qquad m = \frac{[M]}{[M]_0} \qquad f = \frac{[F]}{[M]_0}$$

$$m_i^* = \frac{[M_i^*]}{[M]_0} \ (i \geq 1) \qquad [F] = \sum_{i=s}^{\infty} [M_i^*]$$

Supplementary Equations

$$\frac{dm}{d\tau} = -m\left(\sum_{i=1}^{s-1} m_i^* + \sigma^{-1} f\right) \tag{1}$$

$$\frac{dm_1^*}{d\tau} = -m\, m_1^* \qquad i = 1 \tag{2}$$

$$\frac{dm_i^*}{d\tau} = m(m_{i-1}^* - m_i^*) \qquad 1 < i < s \tag{3}$$

$$\frac{dm_s^*}{d\tau} = m(m_{s-1}^* - \sigma^{-1} m_s^*) \qquad i = s \tag{4}$$

$$\frac{dm_i^*}{d\tau} = \sigma^{-1} m(m_{i-1}^* - m_i^*) \qquad i > s \tag{5}$$

$$\frac{df}{d\tau} = m\, m_{s-1}^* \tag{6}$$

IV. NMR Spectra

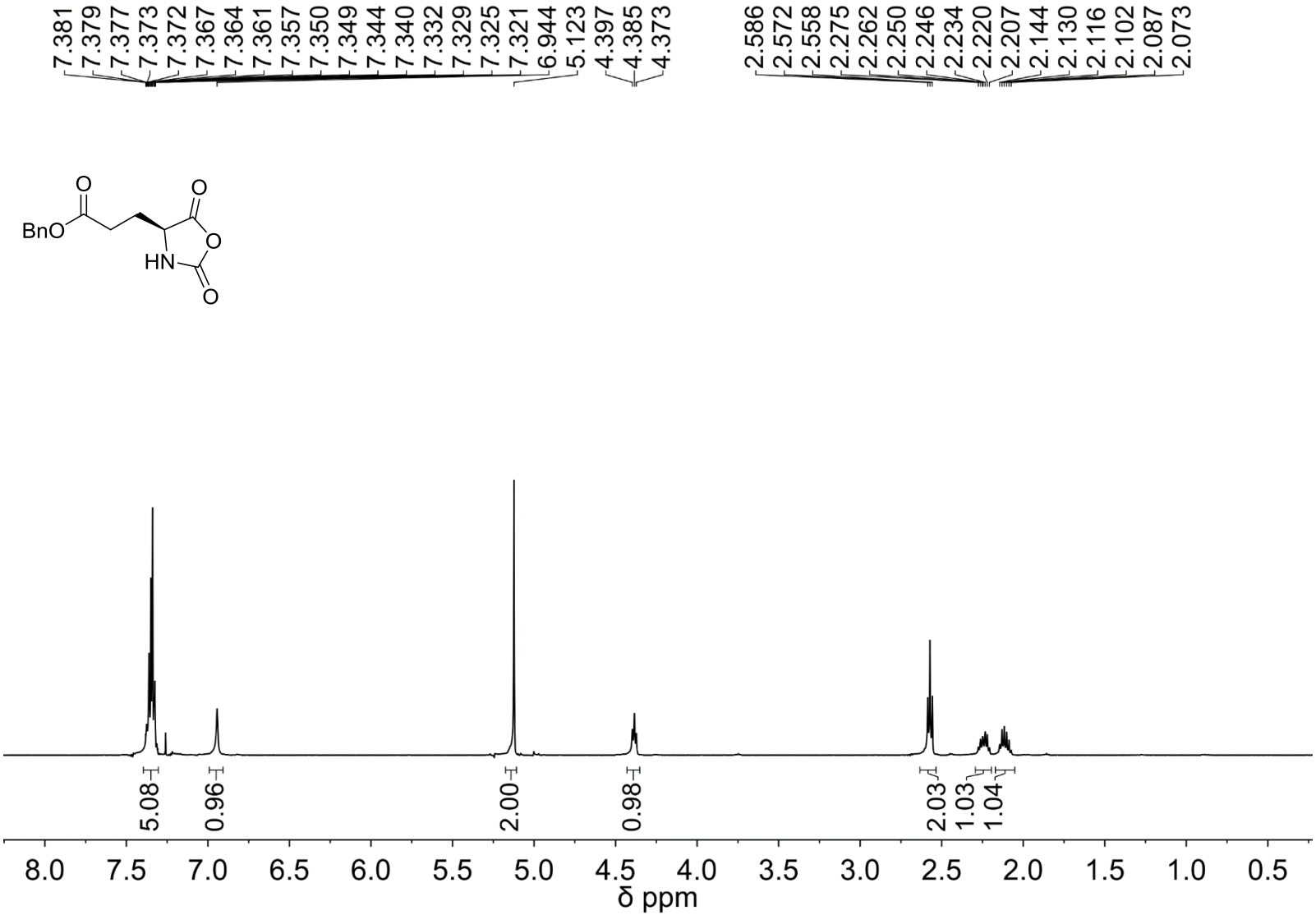

500 MHz, $CDCl_3$

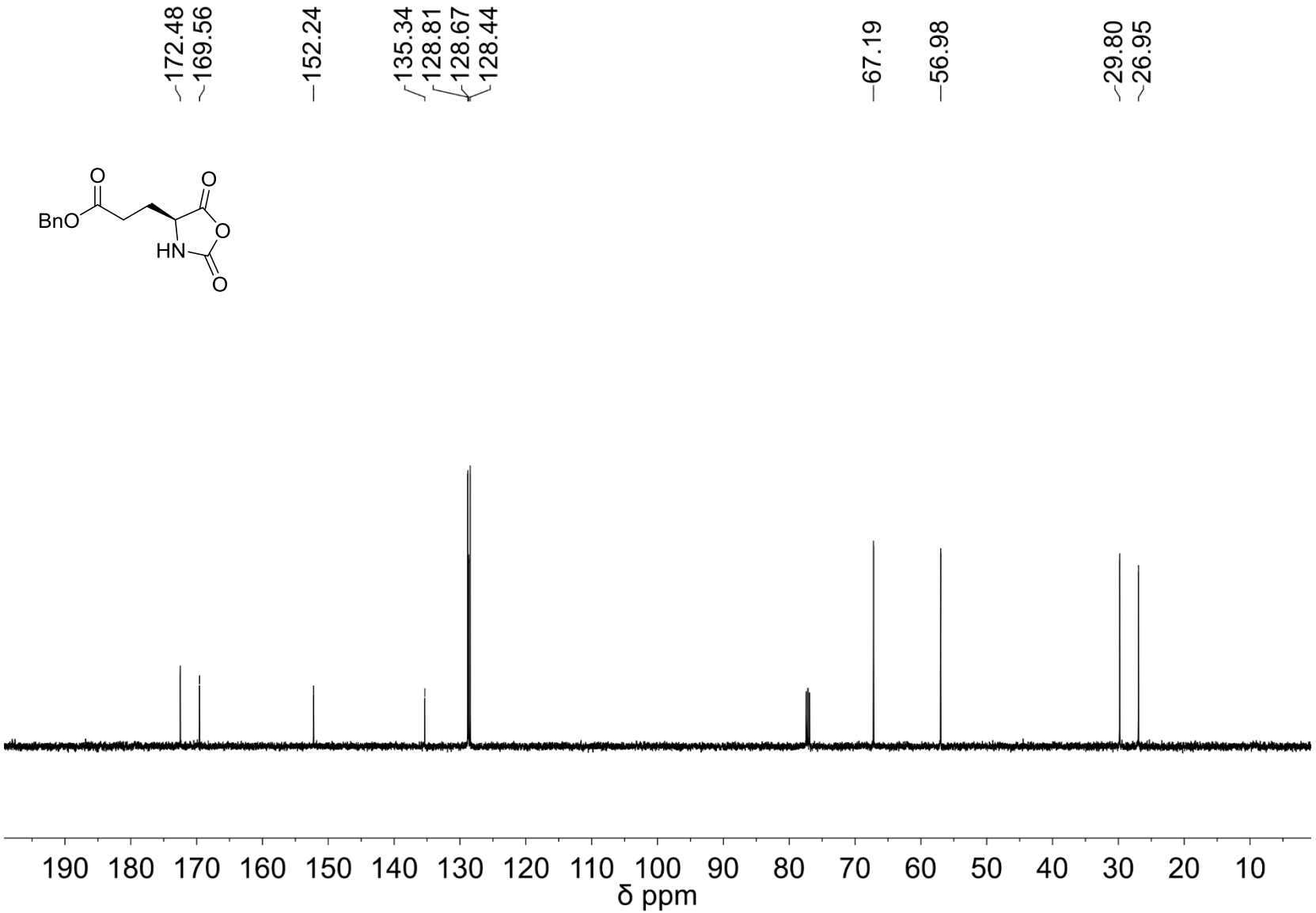

125MHz, $CDCl_3$,

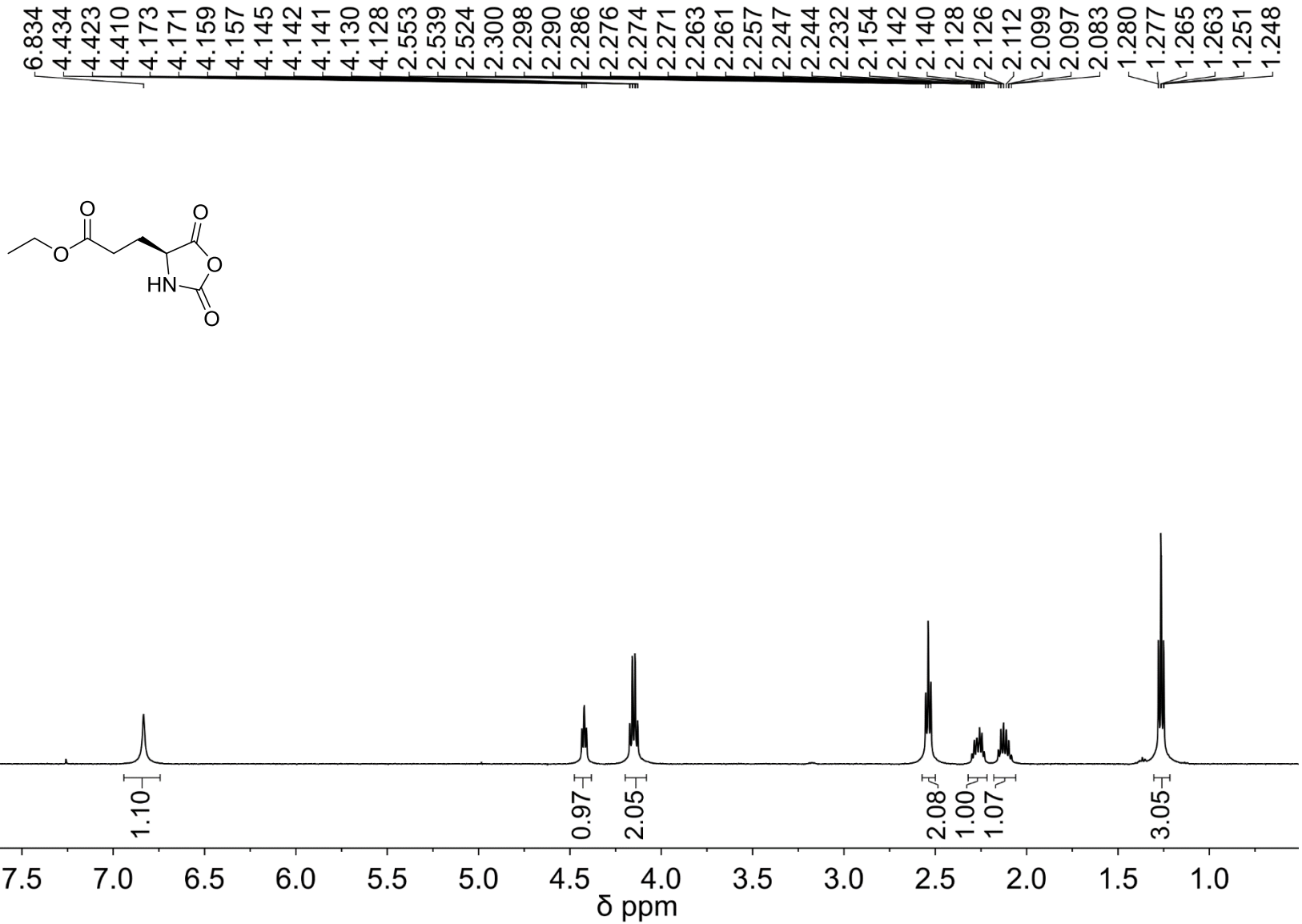

500 MHz, $CDCl_3$

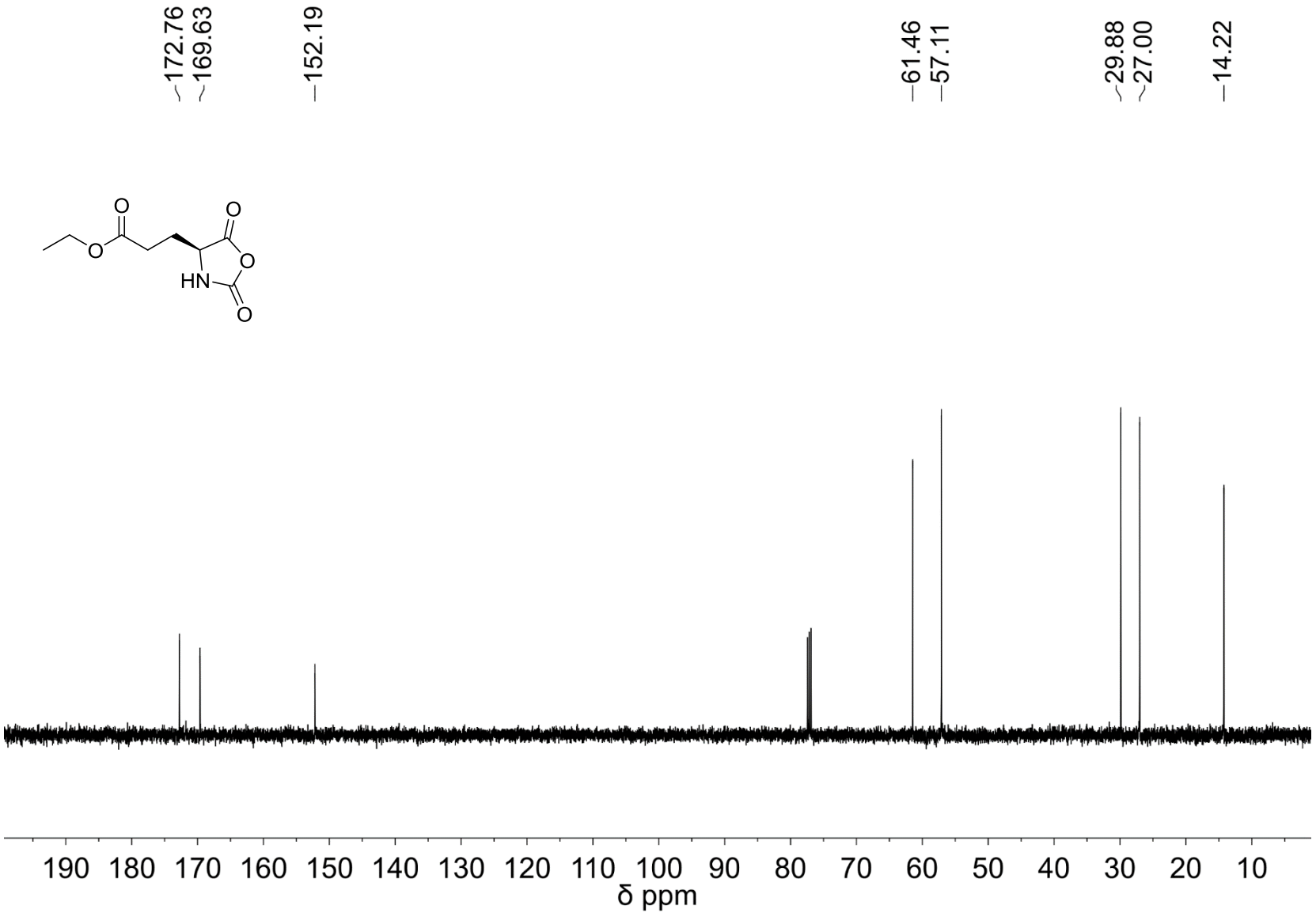

125 MHz, $CDCl_3$

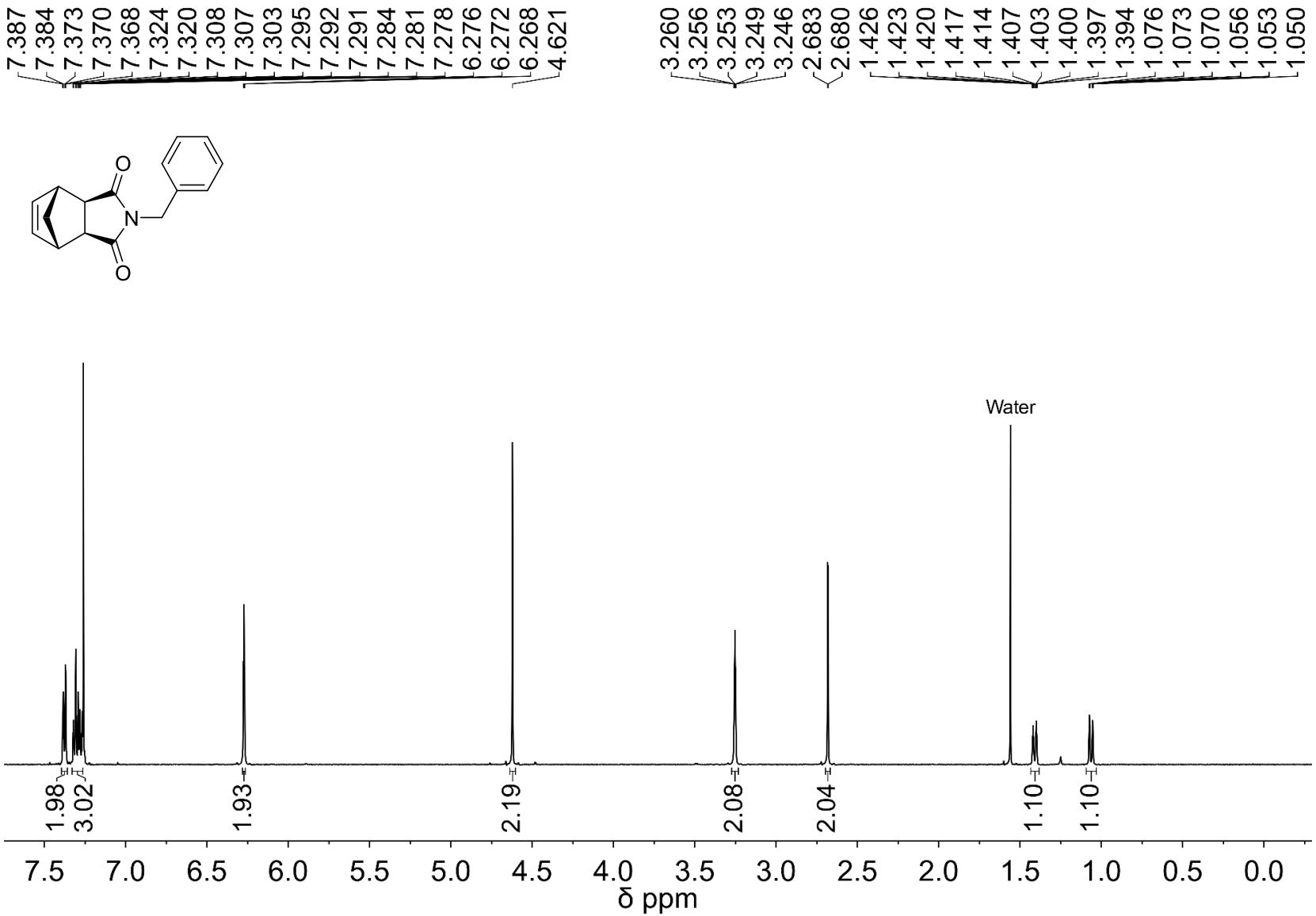

500 MHz, $CDCl_3$

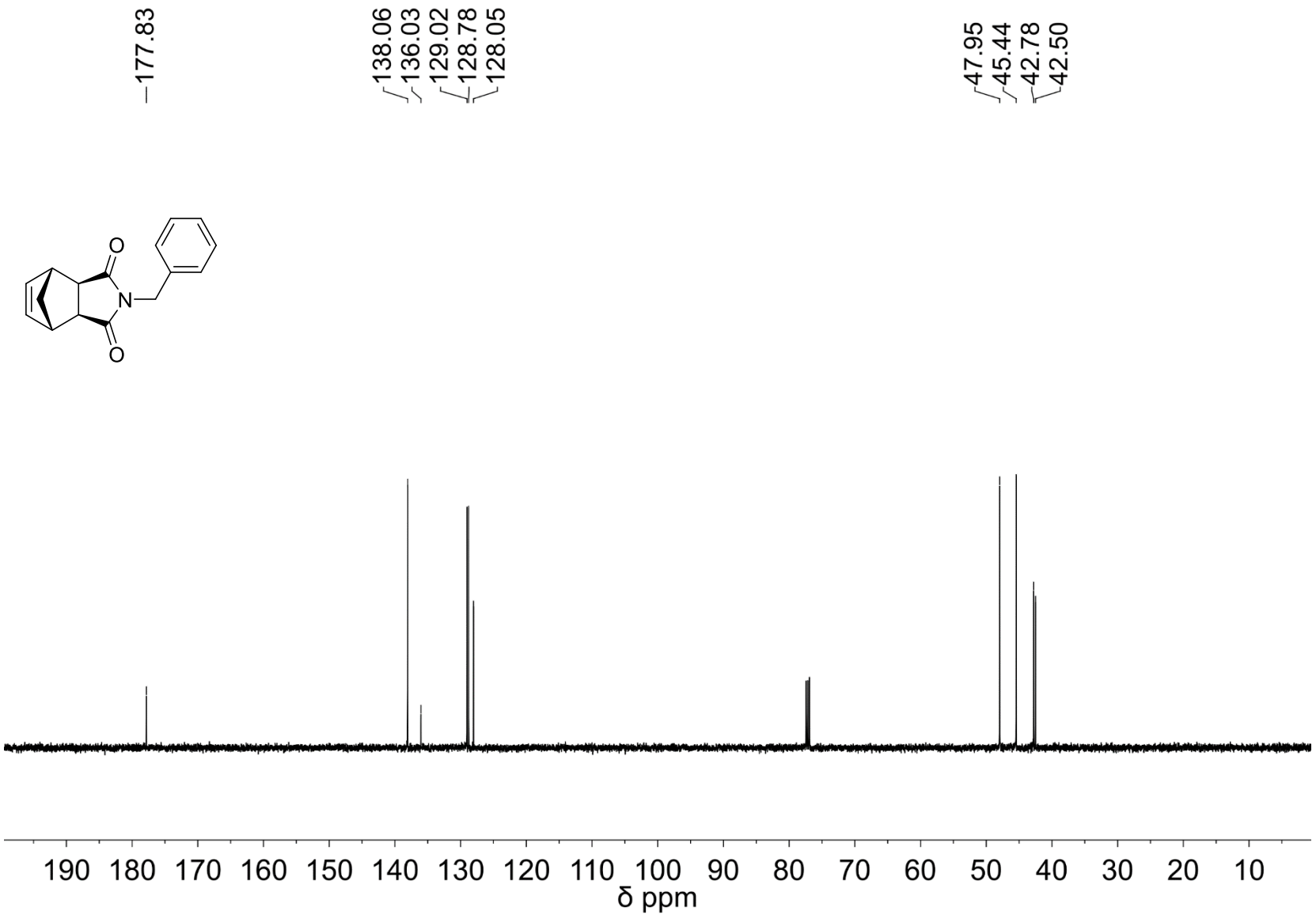

125 MHz, $CDCl_3$

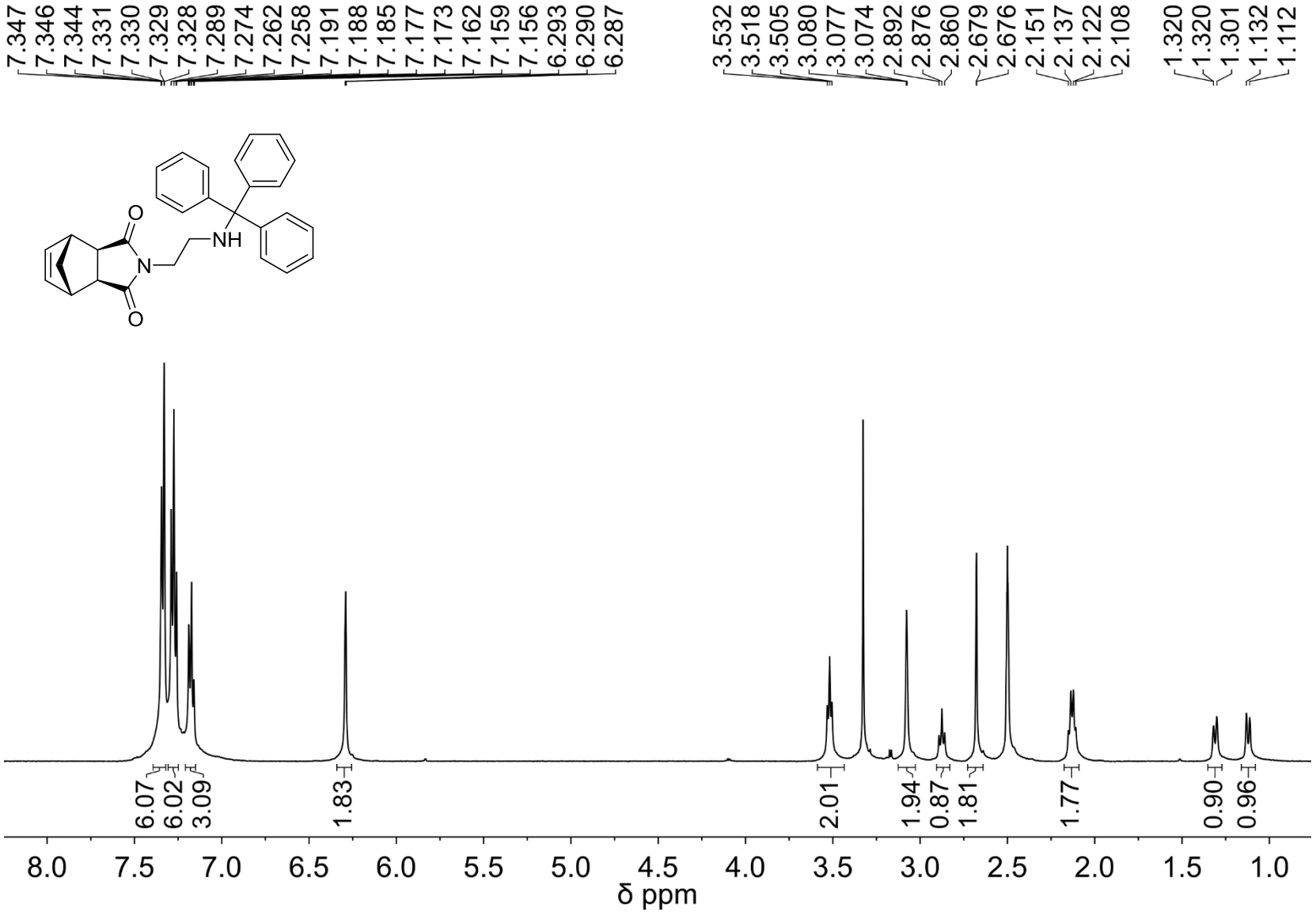

500 MHz, $CDCl_3$

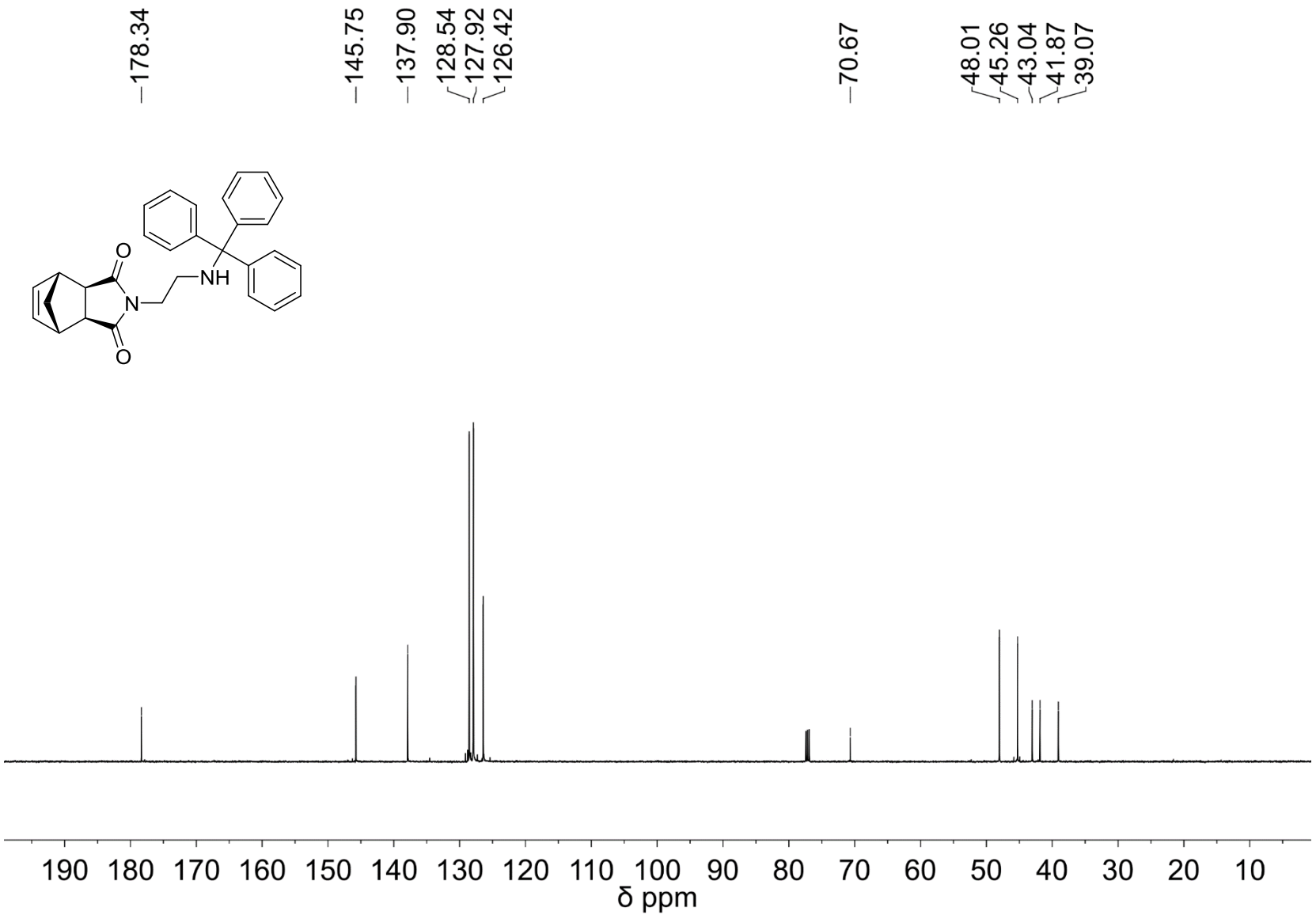

125 MHz, $CDCl_3$

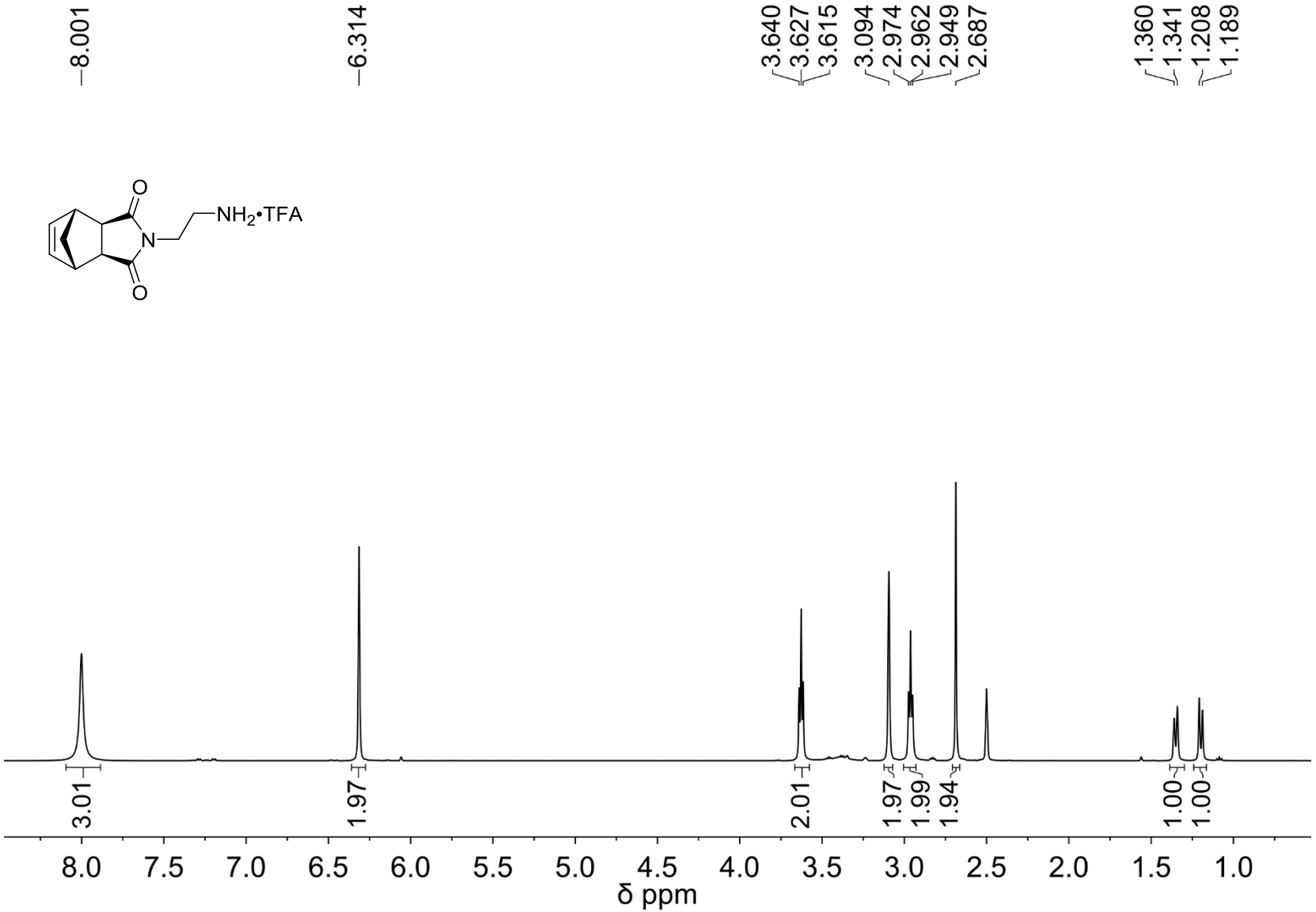

500 MHz, DMSO-d_6

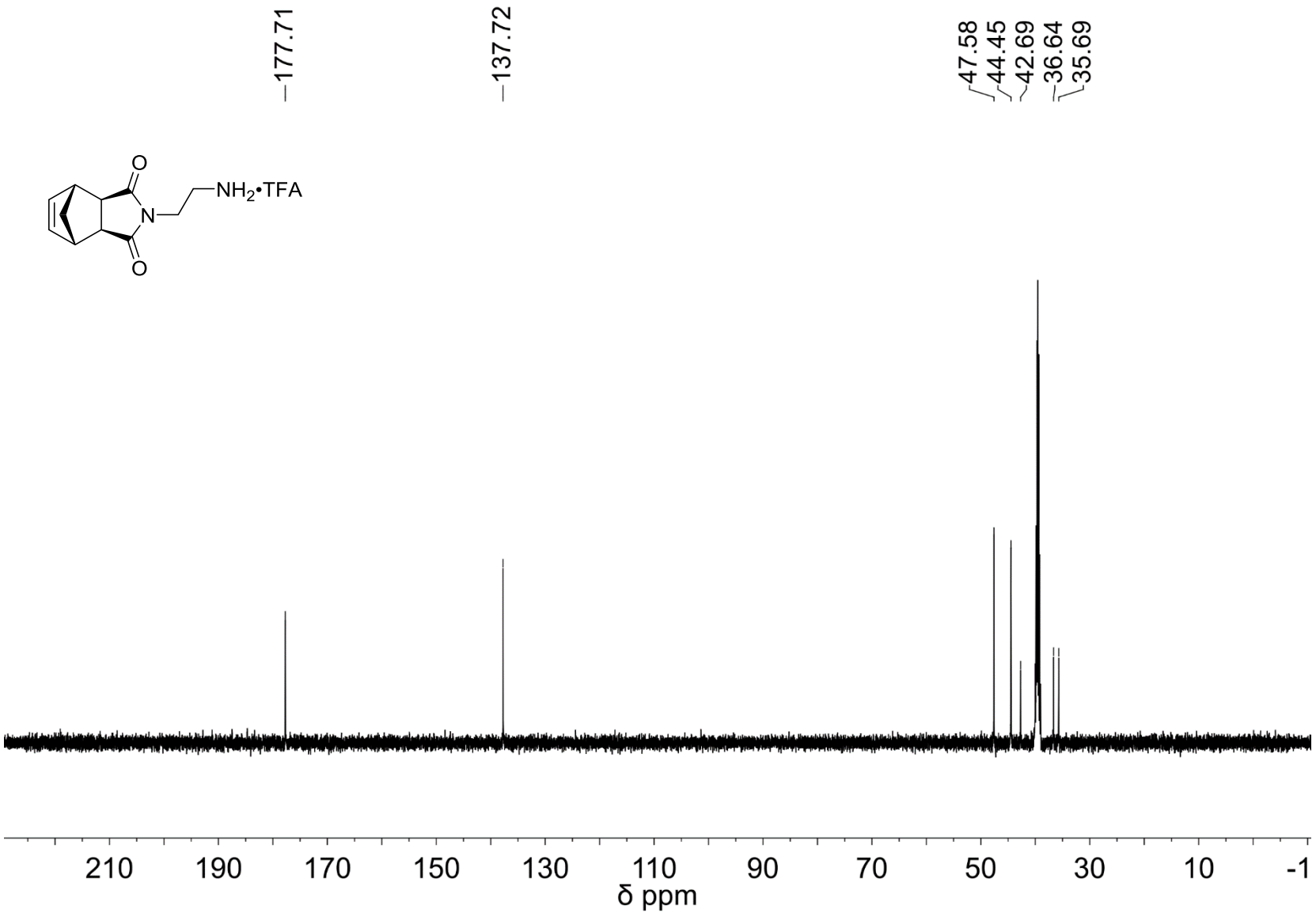

125 MHz, DMSO-d_6

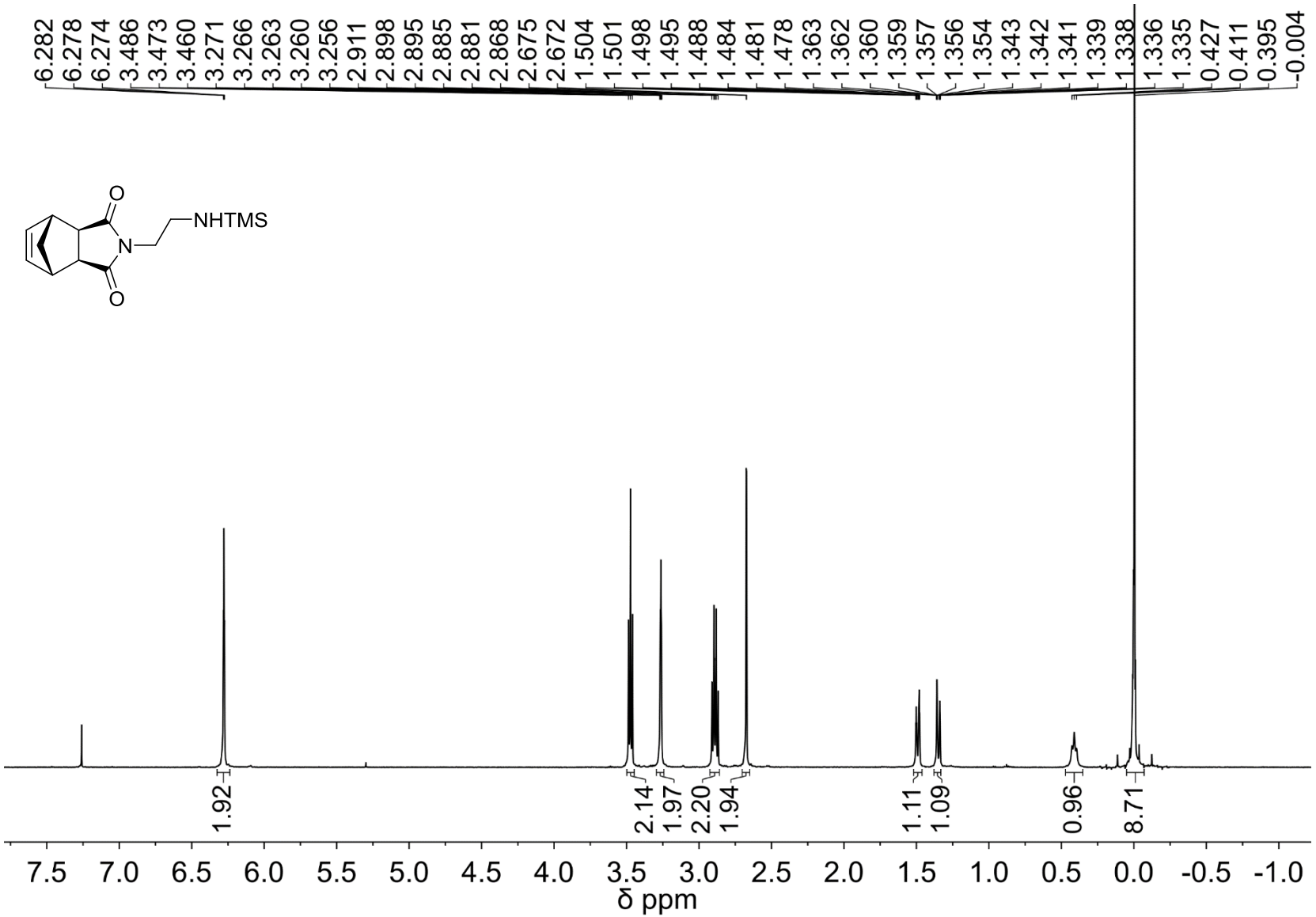

500 MHz, $CDCl_3$

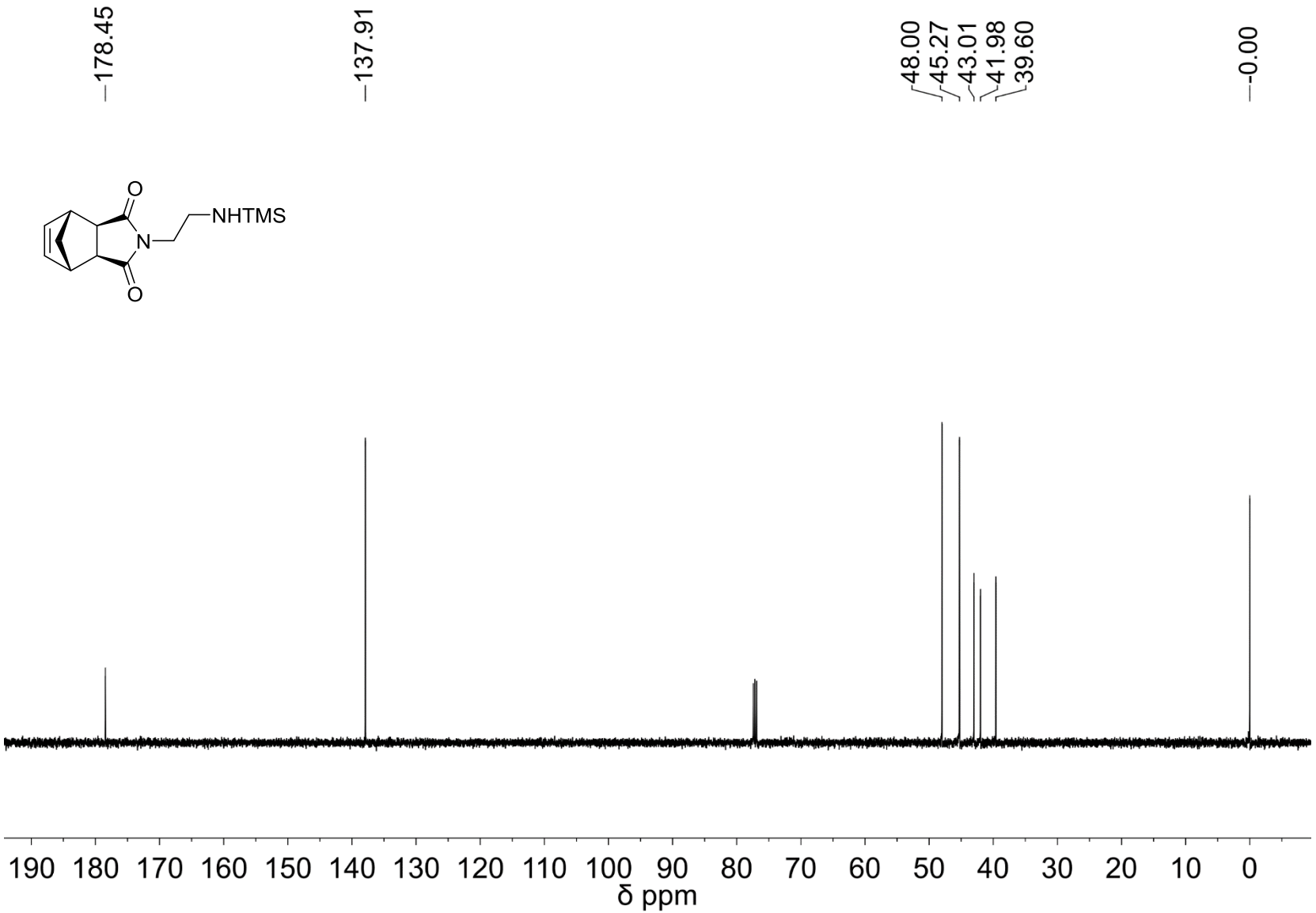

125 MHz, $CDCl_3$

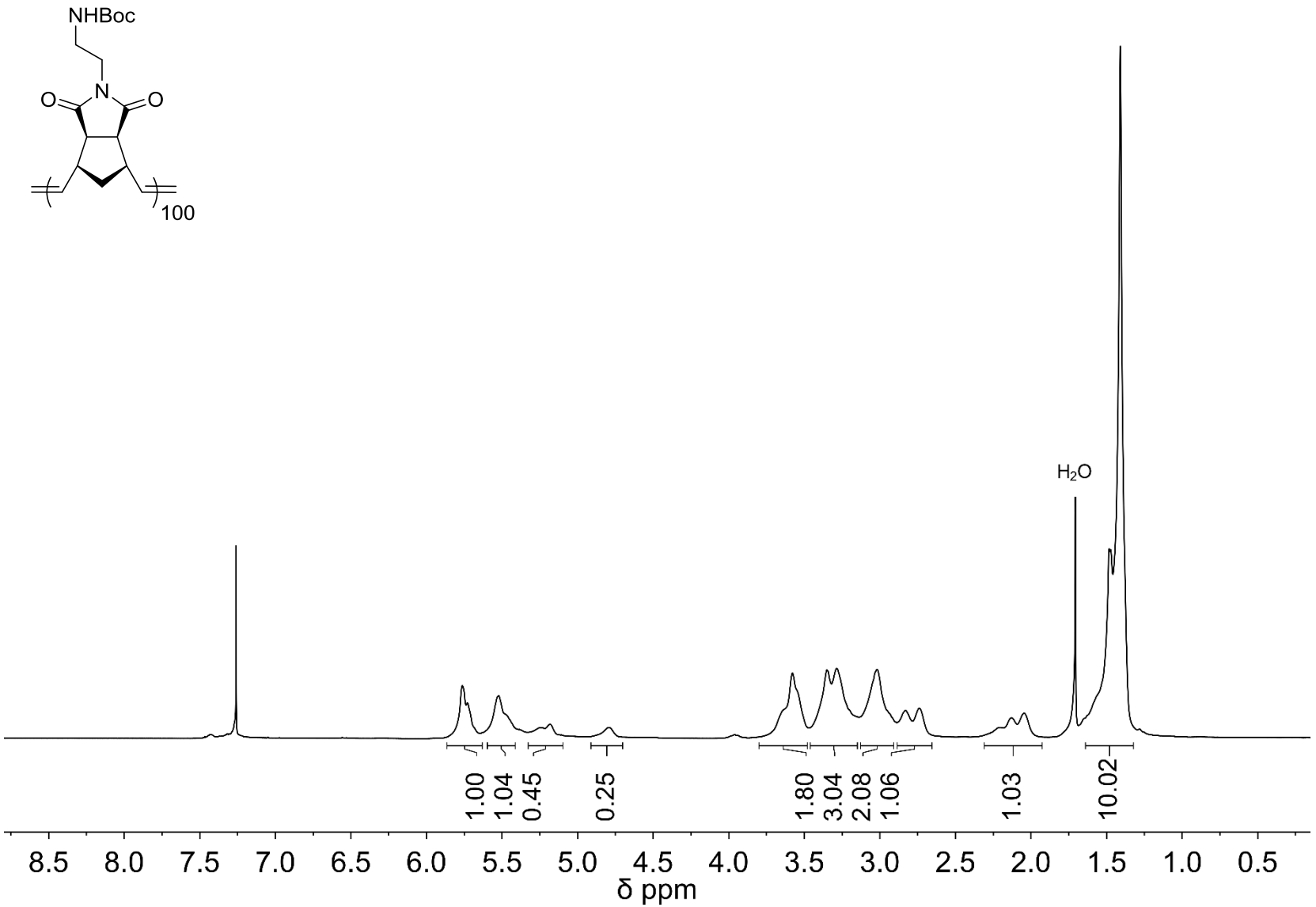

500 MHz, $CDCl_3$

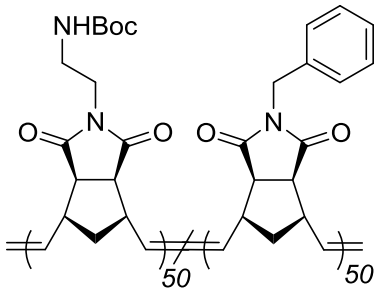

Random

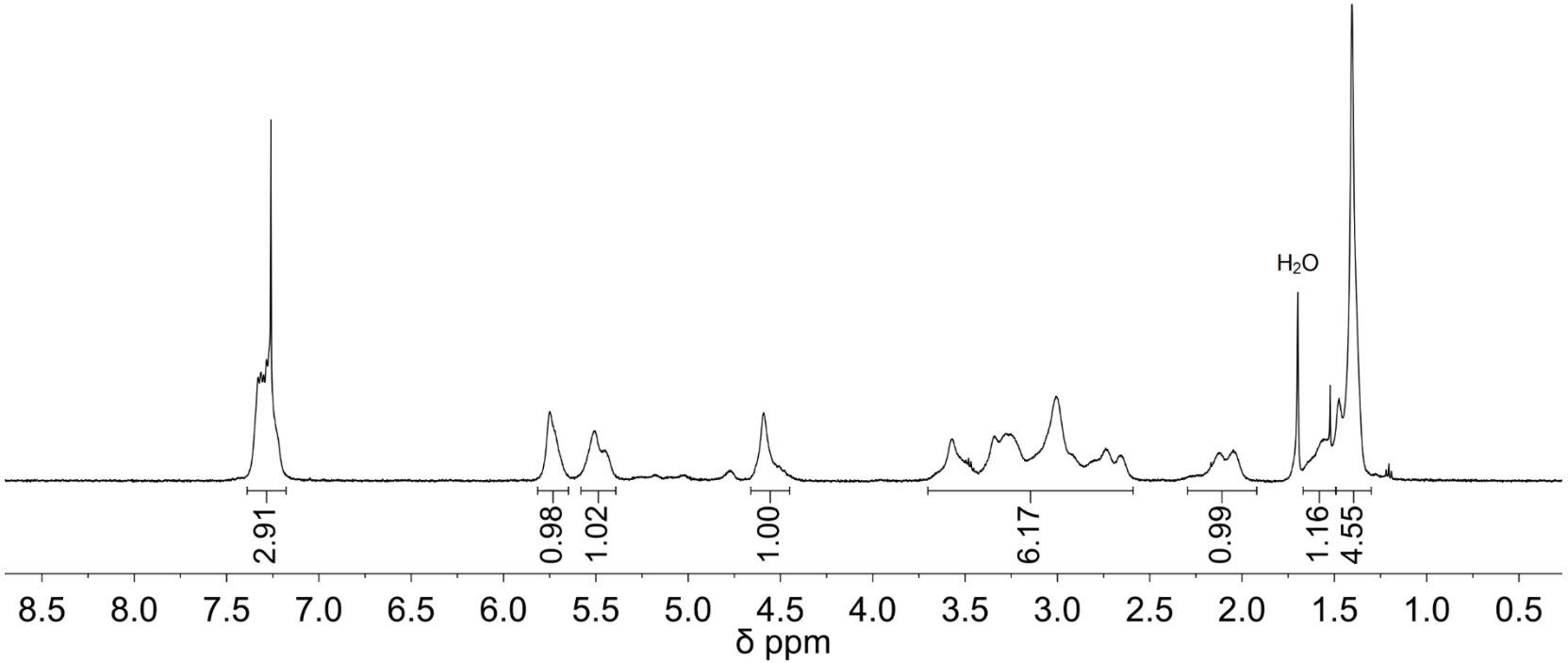

500 MHz, $CDCl_3$

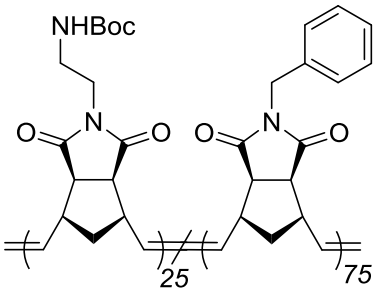

Random

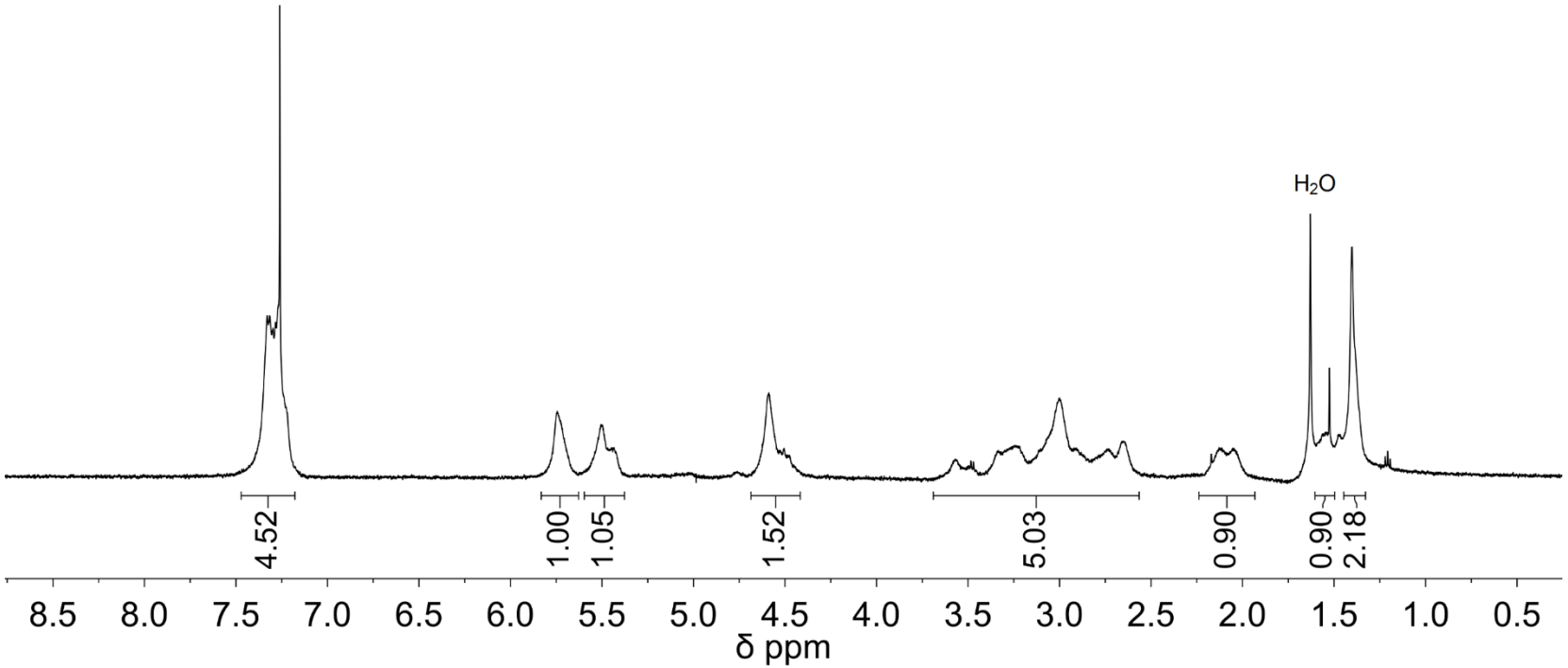

500 MHz, $CDCl_3$

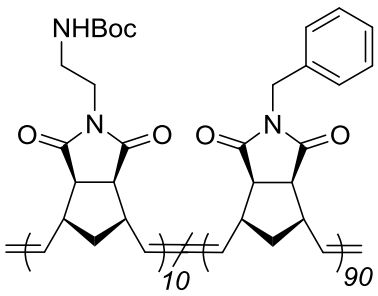

Random

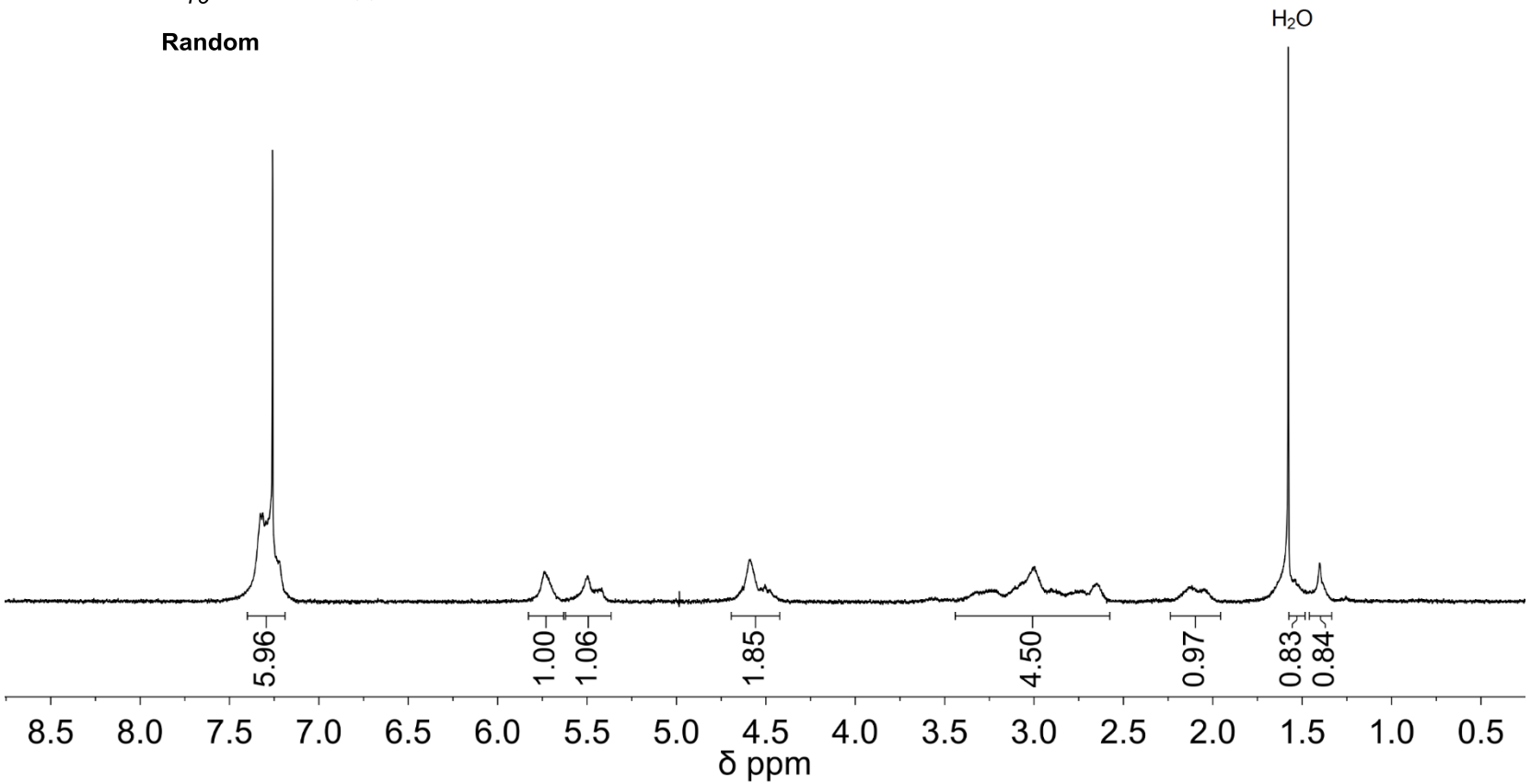

500 MHz, $CDCl_3$

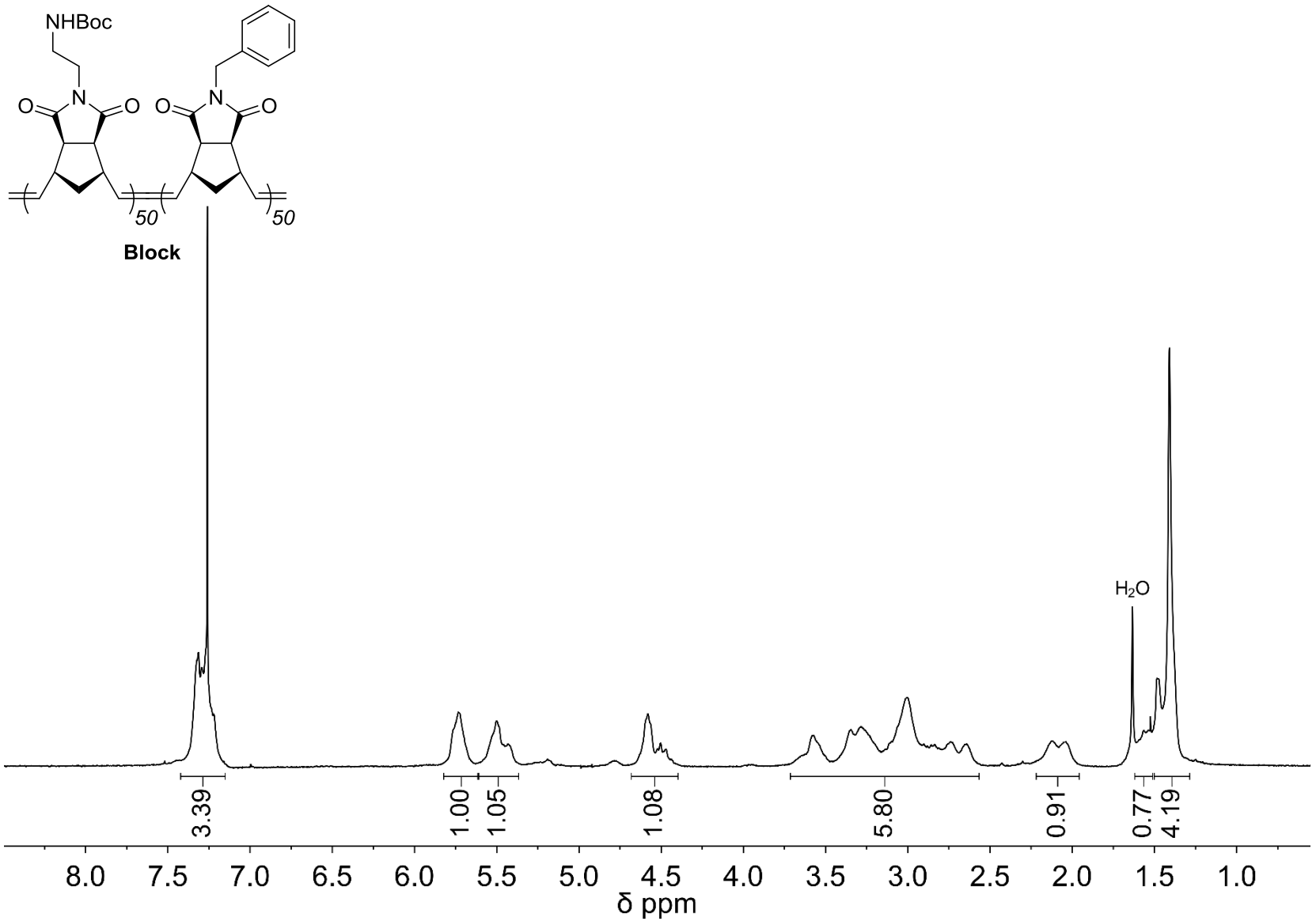

500 MHz, $CDCl_3$

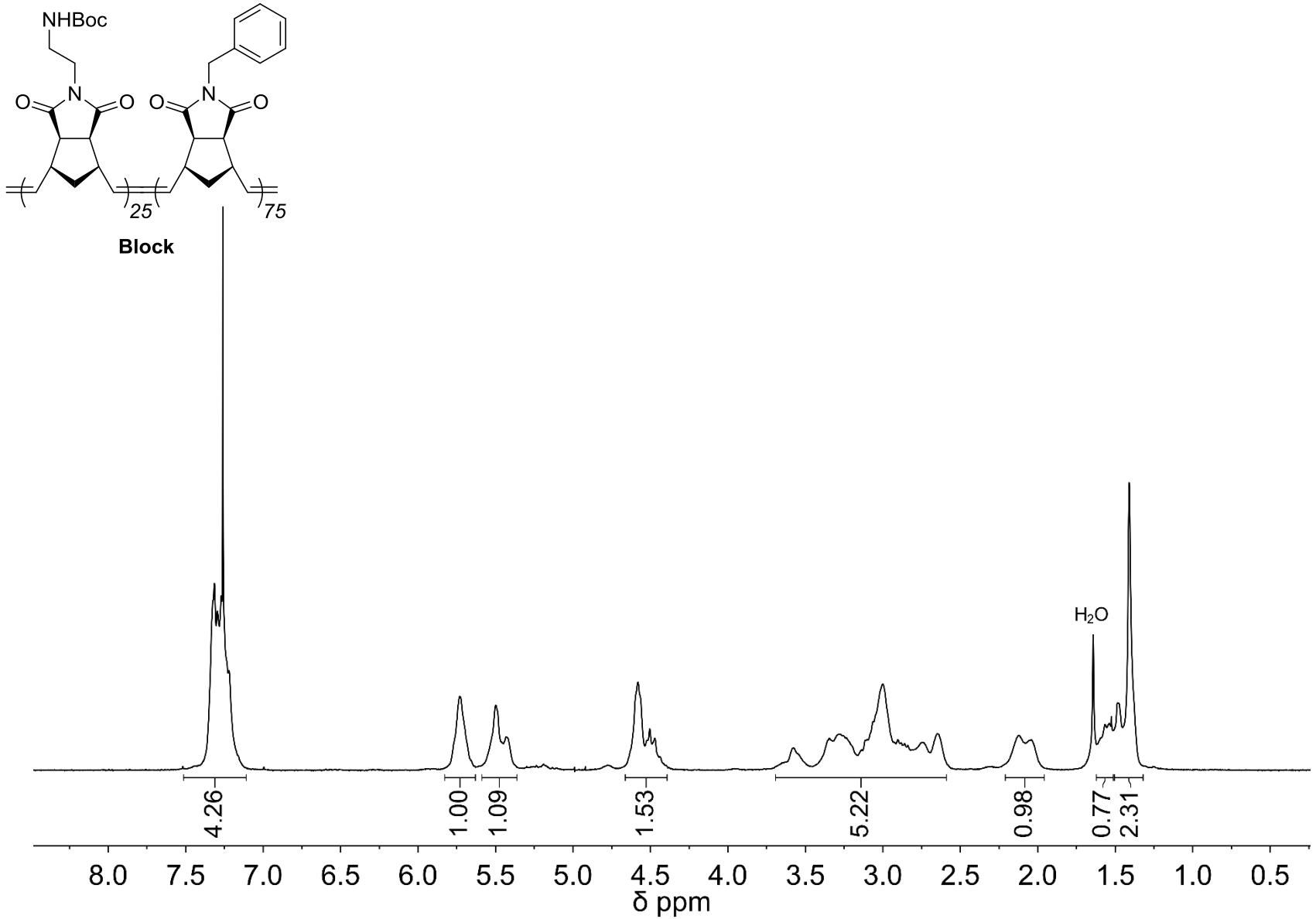

500 MHz, $CDCl_3$

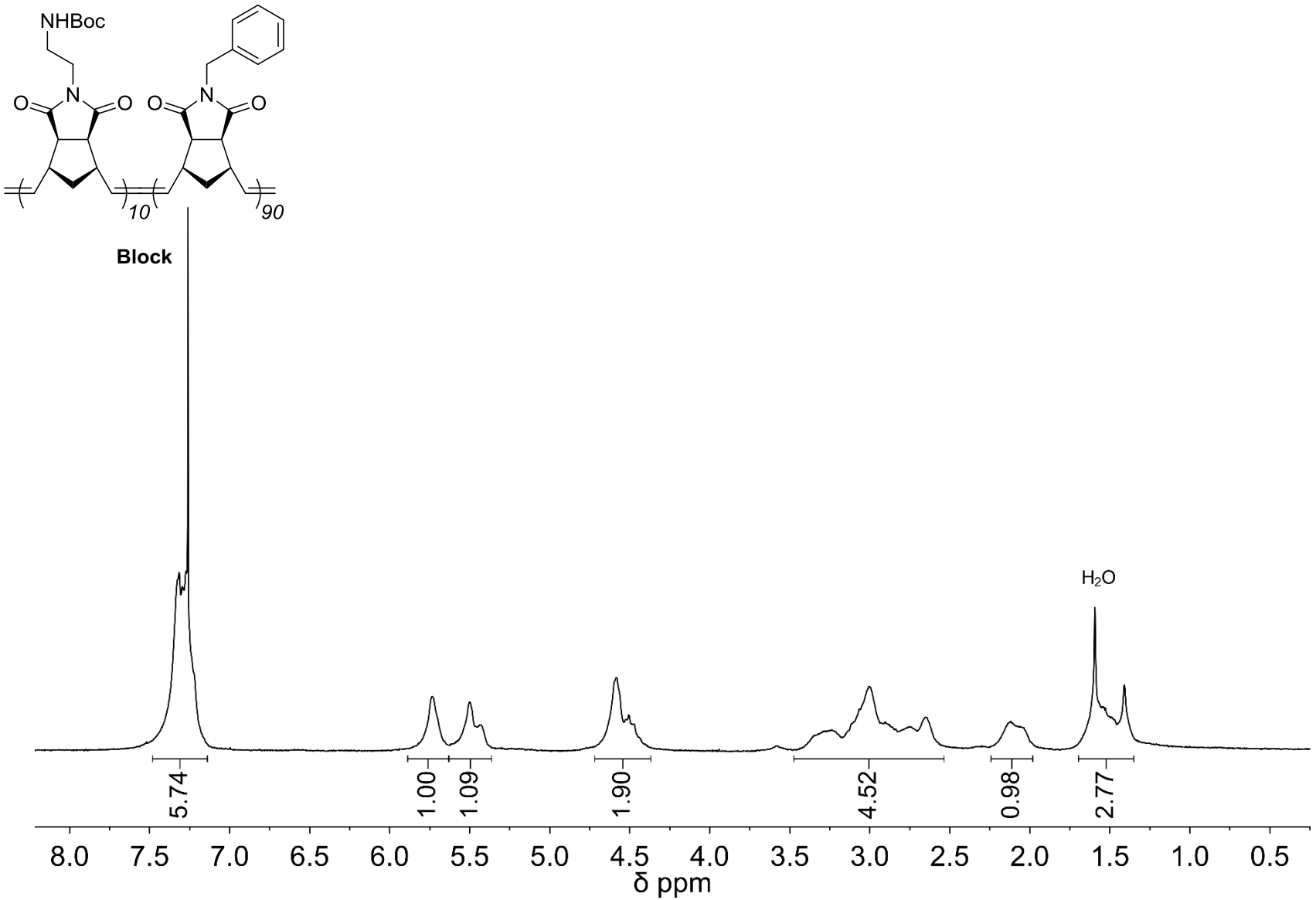

500 MHz, $CDCl_3$

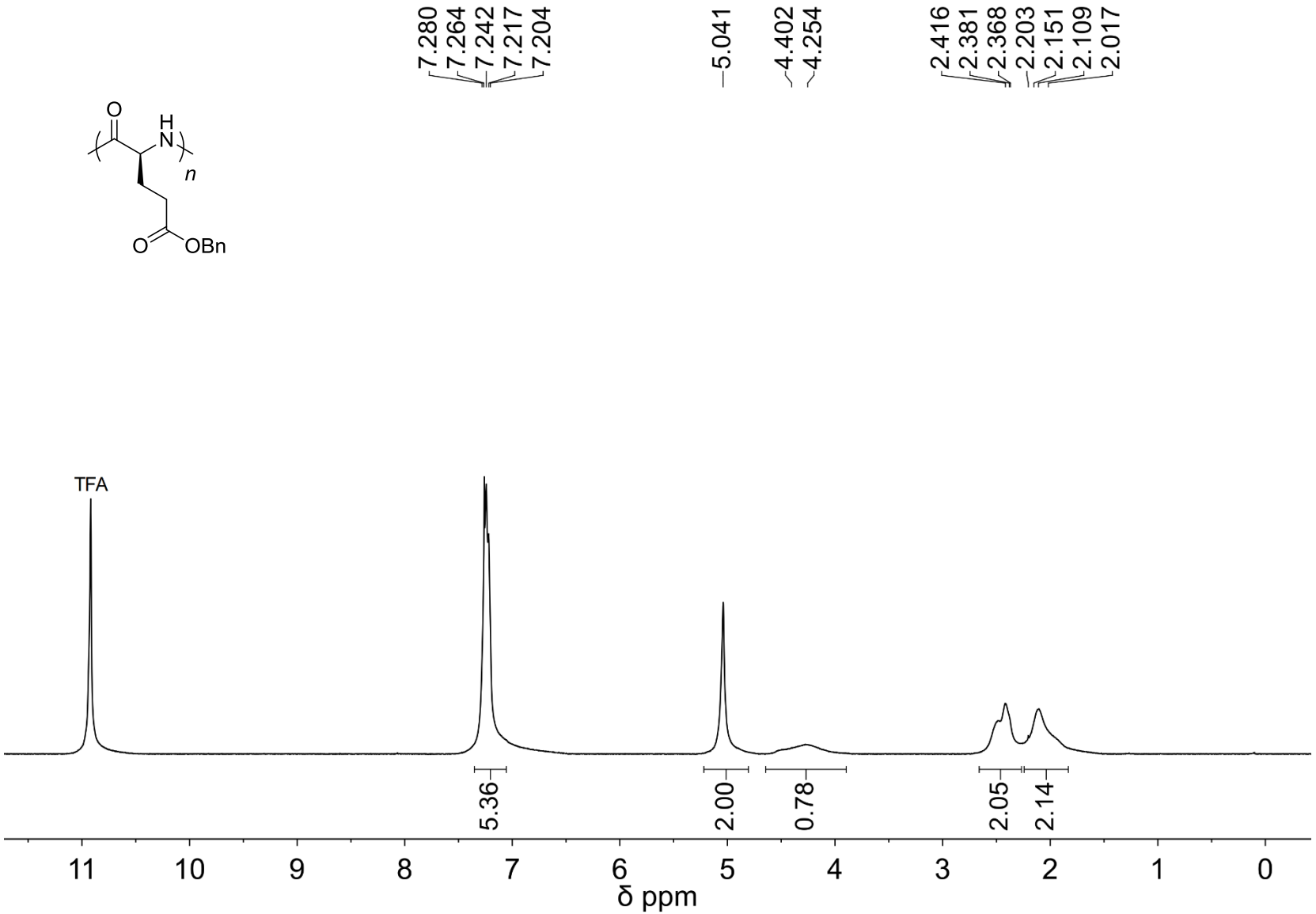

Linear PBLG after ozonolysis of PNB_{100}-*g*-$PBLG_{50}$: 500 MHz, $CDCl_3$:TFA-*d* (9:1, v/v)

1. Sanford, M. S., Love, J. A. & Grubbs, R. H. A versatile precursor for the synthesis of new ruthenium olefin metathesis catalysts. *Organometallics* **20**, 5314-5318 (2001).
2. Tilley, J. W., Levitan, P., Kierstead, R. W. & Cohen, M. Antihypertensive (2-aminoethyl)thiourea derivatives. 1. *J. Med. Chem.* **23**, 1387-1392 (1980).
3. Yu, M., Nowak, A. P., Deming, T. J. & Pochan, D. J. Methylated mono- and diethyleneglycol functionalized polylysines: nonionic, α-helical, water-soluble polypeptides. *J. Am. Chem. Soc.* **121**, 12210-12211 (1999).
4. Gareth Davies, R.*, et al.* Synthesis of nucleic-acid base containing norbornene derivatives as monomers for ring-opening-metathesis-polymerization. *J. Chem. Soc., Perkin Trans. 1*, 3365-3381 (2001).